

**ENERGY LEVELS IN  $\text{Co}^{60}$**

**George Melvin Foglesong**

**and**

**David Guy Foxwell**











8854

on spine:

FUGLESONG

1954

THESIS

F53

Letter on front cover:

ENERGY LEVELS IN Co<sup>60</sup>

George Melvin Foglesong  
and  
David Guy Foxwell





ENERGY LEVELS IN Co<sup>60</sup>

by

George Melvin Foglesong  
" B.S., U.S. Naval Academy  
(1945)

and

David Guy Foxwell  
B.S., U.S. Naval Academy  
(1947)

SUBMITTED IN PARTIAL FULFILLMENT  
OF THE REQUIREMENTS FOR THE DEGREE OF  
MASTER OF SCIENCE

at the

MASSACHUSETTS INSTITUTE OF TECHNOLOGY

June, 1954



## ACKNOWLEDGMENTS

The authors wish to express their gratitude to the members of the High Voltage Laboratory for their constant assistance and cooperation, without which this work could not have been accomplished. We are particularly indebted to Prof. Buechner for proposing and supervising this thesis, and to G. K. Bockelman, G. P. Browne, C. M. Braams, and A. Spurduto for their assistance and helpful suggestions during the course of this work. Finally, thanks are due to those who helped in the tedious business of counting tracks on the photographic plates: W. A. Tripp, Miss Janet Frothingham, Miss Lillian Stone, and Miss Sylvia Darrow.

25053

28842

MEMORANDUM

The subject of this memorandum is the  
 members of the High Voltage Laboratory for their services  
 excellent and commendable, without which this work would  
 not have been accomplished. We are particularly indebted  
 to Prof. [Name] for his generous and unstinting assistance,  
 and to [Name], [Name], [Name], [Name], [Name], and  
 [Name] for their excellent and helpful suggestions  
 during the course of this work. Finally, thanks are due to  
 those who helped in the various matters of routine nature  
 in the photographic division. It is with these thanks  
 that I close, and I am, Sir, very truly,  
 Yours faithfully,

## TABLE OF CONTENTS

	Page
ACKNOWLEDGMENTS	
ABSTRACT	
I. INTRODUCTION	1
II. DESCRIPTION OF APPARATUS AND TARGET PREPARATION	6
A. Apparatus	6
B. Target Preparation	12
III. EXPERIMENTAL PROCEDURE	15
IV. RESULTS AND CONCLUSIONS	27
A. Probable Error	27
B. Results	34
C. Comparison with Previous Results	36
D. Conclusion	36
APPENDIX A	42
BIBLIOGRAPHY	44

STATUTES OF THE

1887

1. The Statute in relation to the... 1

2. The Statute in relation to the... 2

3. The Statute in relation to the... 3

4. The Statute in relation to the... 4

5. The Statute in relation to the... 5

6. The Statute in relation to the... 6

7. The Statute in relation to the... 7

8. The Statute in relation to the... 8

9. The Statute in relation to the... 9

10. The Statute in relation to the... 10

11. The Statute in relation to the... 11

12. The Statute in relation to the... 12

13. The Statute in relation to the... 13

14. The Statute in relation to the... 14

15. The Statute in relation to the... 15

16. The Statute in relation to the... 16

17. The Statute in relation to the... 17

18. The Statute in relation to the... 18

19. The Statute in relation to the... 19

20. The Statute in relation to the... 20



# ENERGY LEVELS IN $\text{Co}^{60}$

by

George Melvin Foglesong  
Lieutenant, U. S. Navy

and

David Guy Foxwell  
Lieutenant, U. S. Navy

Submitted to the Department of Physics on May 24, 1954 in  
partial fulfillment of the requirements for the degree of  
Master of Science

## A B S T R A C T

Proton groups from the reaction  $\text{Co}^{59}(d,p)\text{Co}^{60}$  were examined in order to determine the ground state  $Q$ -value and the excitation energies of the lower lying excited states of  $\text{Co}^{60}$ . Platinum-backed naturally mono-isotopic cobalt targets were bombarded with magnetically analysed deuteron beams from the MIT-CNR Van de Graaff generator, and the protons emerging at  $90^\circ$  to the incident beam were analysed by a  $180^\circ$  focusing magnetic spectrograph and photographically detected.

The targets were made by vacuum evaporating cobalt pellets onto platinum sheets cleaned with hydrochloric acid. The high boiling point of cobalt required the use of a technique of pinching the pellets between sharpened carbon electrodes. Spectro-chemical analysis of the cobalt showed impurities of nickel, magnesium, and copper, with lesser amounts of other metals. Known levels in nickel and magnesium could be identified with smaller proton groups, but, owing to the rather high background and density of levels, not conclusively. Levels assigned to cobalt were confirmed by noting the variation of the proton group energies with deuteron energy. Bombarding energies of 5.0 and 5.8 Mev were used.

The ground state  $Q$ -value was measured as  $5.280 \pm 0.008$  Mev. The metastable state, observed in beta- and gamma-ray decay measurements at  $58.5 \pm .5$  kev and seen here for the first time in any nuclear reaction, was measured as  $60 \pm 3$  kev. Other low lying excited states agree with those previously determined by  $(n, \gamma)$

REPORT OF THE

AND

COMMISSIONERS OF THE

LAND

OFFICE

IN REGARD TO THE

LANDS BELONGING TO THE

STATE OF

ALABAMA

Presented to the Senate of the State of Alabama, in the year 1845, by the Honorable John A. Quitman, Governor of the State.

By the Honorable John A. Quitman, Governor of the State, and the Honorable Commissioners of the Land Office.

Printed by the State Printer, in the year 1845.



reactions, and further identify the most energetic gamma-ray seen in these reactions as being that to the ground state of  $\text{Co}^{60}$ . The higher excited states, while in poor agreement with the corresponding  $(n, \gamma)$  results, showed a complex level structure, as was expected for this odd-odd nucleus, and as was indicated in the  $(n, \gamma)$  work.

Thesis Supervisor: W. F. Buchner

Title: Associate Professor of Physics

THE UNIVERSITY OF CHICAGO  
DEPARTMENT OF CHEMISTRY  
5800 S. DICKINSON DRIVE  
CHICAGO, ILLINOIS 60637  
(773) 936-3100

RECEIVED AT THE UNIVERSITY OF CHICAGO

LIBRARY OF CHEMISTRY

DATE RECEIVED: 10/15/1964

BY: [Name]

LIBRARY USE ONLY

10/15/1964

1. [Faint text]

2. [Faint text]

3. [Faint text]

### I. INTRODUCTION

M.I.T. Van de Graaff generators have been used extensively over the past few years to obtain precise information on the nuclear energy levels of various light and intermediate nuclei. These accelerators, when coupled with magnetic momentum analyzers and magnetic spectrographs, provide data of a high degree of accuracy and resolution. The concentration of effort has been on light nuclei, where it is felt that the relatively few nucleons should lend themselves to a detailed treatment of nuclear forces, particularly if some of them can be grouped into closed shells. The emergence of isobaric polyad structure has supported the idea of charge independence of nuclear forces, but, to date, only limited success has been achieved in the formulation of a theory of nuclear forces.

The completion of a new accelerator, designated the MIT-CNR Van de Graaff generator, about two years ago extended the available bombarding energy from 2.0 Mev to 8.5 Mev and opened up the possibility of accurate measurements of the energy levels of heavy nuclei. Two specific problems dealing with naturally mono-isotopic nuclei were suggested to the authors by Dr. W. W. Buechner:

1. INTRODUCTION

It is well known that the energy levels of a system are determined by the potential energy function. In the case of a harmonic oscillator, the energy levels are equally spaced. However, in the case of an anharmonic oscillator, the energy levels are not equally spaced. This is due to the fact that the potential energy function is not a simple harmonic function. The anharmonicity of the potential energy function leads to a non-linear relationship between the energy levels and the quantum number. This is the case for the Morse potential, which is a common model for the potential energy of a diatomic molecule. The Morse potential is given by the equation  $V(x) = D_e(1 - e^{-ax})^2$ , where  $D_e$  is the dissociation energy and  $a$  is a constant. The energy levels of the Morse potential are given by the equation  $E_n = D_e - \frac{1}{2}hc\omega_e(x_e - n)^2$ , where  $\omega_e$  is the harmonic frequency and  $x_e$  is the equilibrium internuclear distance. This equation shows that the energy levels are not equally spaced, and that they approach a limit as the quantum number increases. This is the case for the Morse potential, which is a common model for the potential energy of a diatomic molecule. The energy levels of the Morse potential are given by the equation  $E_n = D_e - \frac{1}{2}hc\omega_e(x_e - n)^2$ , where  $\omega_e$  is the harmonic frequency and  $x_e$  is the equilibrium internuclear distance. This equation shows that the energy levels are not equally spaced, and that they approach a limit as the quantum number increases.

The energy levels of a diatomic molecule are determined by the potential energy function. In the case of a harmonic oscillator, the energy levels are equally spaced. However, in the case of an anharmonic oscillator, the energy levels are not equally spaced. This is due to the fact that the potential energy function is not a simple harmonic function. The anharmonicity of the potential energy function leads to a non-linear relationship between the energy levels and the quantum number. This is the case for the Morse potential, which is a common model for the potential energy of a diatomic molecule. The energy levels of the Morse potential are given by the equation  $E_n = D_e - \frac{1}{2}hc\omega_e(x_e - n)^2$ , where  $\omega_e$  is the harmonic frequency and  $x_e$  is the equilibrium internuclear distance. This equation shows that the energy levels are not equally spaced, and that they approach a limit as the quantum number increases.



(1) The apparent 0.4 Mev discrepancy in the following cycle<sup>1</sup> of ground state Q-values and decay energies which would most logically be attributed<sup>2</sup> to an incorrect assignment of the ground state of Bi<sup>210</sup>: Pb<sup>206</sup>, Fb<sup>207</sup>, Fb<sup>208</sup>, Pb<sup>209</sup>, Bi<sup>209</sup>, Bi<sup>210</sup>, Po<sup>206</sup>; and,

(2) The indeterminacy of the location of the ground state of Co<sup>60</sup> in relation to the excited states of Co<sup>60</sup> as given by Bartholomew and Kinsey,<sup>3</sup> and the questionable spin assignments of the ground and first excited states of this nucleus.<sup>4</sup>

While the first problem was not solved because of a temporary reduction in the maximum attainable voltage with the MIT-ONR generator, tentative results were promising. In pursuing the Bi<sup>209</sup>(d,p)Bi<sup>210</sup> reaction, preliminary results with a bombarding energy of 8 Mev indicated that previously reported proton groups corresponding to the excited states of Bi<sup>210</sup> could be resolved, and the question of the ground state might well be answered by this approach.

Investigation of the second problem did not require such a high bombarding energy. The most reliable source of information on energy levels in Co<sup>60</sup> lies in the (n, γ) work of Bartholomew and Kinsey.<sup>3</sup> While their results indicate relative positions of the excited states, they cannot determine whether their lowest state is attributable to the actual

(1) The present U.S. program in the following  
 state of affairs which are being carried out  
 would most likely be similar to an investment  
 of the funds of the U.S. in the U.S. and  
 in the U.S. and in the U.S. and in the U.S.  
 (2) The importance of the location of the  
 state of CO<sub>2</sub> in relation to the other states of CO<sub>2</sub>  
 given by Barlow and others, and the possibility  
 that the state of CO<sub>2</sub> and the other states of CO<sub>2</sub>  
 this means.  
 While the first problem was not solved because of a  
 temporary reduction in the amount of energy which  
 the U.S. generator, relative to the other  
 in terms of the U.S. and the U.S. and the U.S.  
 results in a combined energy of 1000 units  
 previously reported from other sources corresponding to the  
 relative state of CO<sub>2</sub> could be resolved, and the possibility  
 of the present state will be covered by this program.  
 Investigation of the present program and the results  
 a new program energy. The new relative amount of  
 information on energy levels in CO<sub>2</sub> in the U.S.  
 now of Barlow and others. While their results indicate  
 relative position of the other states, they were not  
 also their relative level of energy in the U.S.

ground state or to the well-known metastable state at  $58.9 \pm 5$  keV<sup>5</sup>. Previous Co<sup>60</sup>(d,n) analyses, by Bateson and Pollard<sup>6</sup>, Hoesterey<sup>7</sup>, and Harvey<sup>1</sup>, had resulted in ground state assignments in which the ground and first excited states were not resolved. This earlier work had been done with cyclotron deuterons and aluminum foils, and was, by its nature, of moderate accuracy and poor resolution.

The question of the spin assignments of the ground and first excited states was brought up recently by the discovery of a new beta-ray from the ground state of Co<sup>60</sup> to the first excited state of Ni<sup>60</sup> as is shown in Figure 1. Keister and Schmidt<sup>4</sup> were led by the shape of the Kurie plot of this beta to the spin and parity assignments of  $4+$  and  $1+$  to the ground and metastable states of Co<sup>60</sup>, respectively, in contrast to the generally accepted values of  $5+$  and  $2+$ . These new assignments, however, cannot be reconciled with the lack of beta decay from the first excited state of Co<sup>60</sup> to the ground state of Ni<sup>60</sup>. This question might have been resolved by using the rotatable magnetic spectrograph currently under development for use in conjunction with the MIT-OMR generator. The angular distribution of the protons and, from Butler's theory<sup>9</sup>, the orbital angular momentum of the captured neutrons might have led to unambiguous spin assignments, as is outlined in Appendix A. Unfortunately, the new spectro-







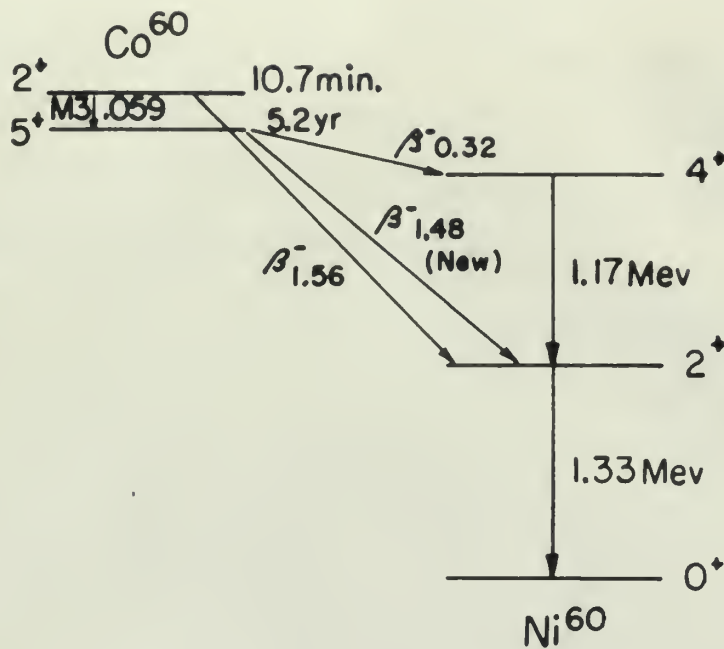


Figure 1

ENERGY LEVEL DIAGRAM SHOWING  
DECAY SCHEME OF  $Co^{60}$



graph was not completed in time to include such an analysis in this work.

The problem, then, was to determine the Q-value of the  $\text{Co}^{59}(\text{d},\text{p})\text{Co}^{60}$  reaction to the ground state of  $\text{Co}^{60}$ , with a secondary purpose of checking the levels of excitation against those previously seen, particularly those levels about which Bartholomew and Kinsey were in doubt.

... ..

... ..

... ..

... ..

... ..

... ..

... ..

## II. DESCRIPTION OF APPARATUS AND TARGET PREPARATION

### A. APPARATUS

The MIT-CNR Van de Graaff generator, used as the source of deuterons for the  $\text{Co}^{59}(\text{d},\text{p})\text{Co}^{60}$  reaction, is shown schematically in Figure 2. Its salient features include a pressurized tank designed for 400 psi, two 18 foot accelerating tubes (of one-inch-thick glass), a string controlled RF ion source capable of ionizing hydrogen, deuterium, or helium, a focus voltage supply capable of providing 40-80 kv, and a controlled corona discharge grid. The deuteron beam is deflected through  $90^\circ$  by an analyzing magnet, after which it strikes the target in the spectrograph (Figure 3).

The energy of the deuteron beam is defined and controlled by means of a one mm slit 90 cm above the analyzing magnet and a 1/2 mm slit 185 cm beyond the analyzing magnet. A given magnetic field in the analyzer determines the momentum of a charged particle which will pass through the slit system. The difference between the currents to the upper and lower exit slits is amplified and this signal is used to control the voltage in the corona discharge grid, thus providing terminal voltage control. This control is satisfactory for terminal voltages down to about 4.5 Mev. The analyzing magnet can be rotated about a vertical axis so as

11. CHARACTERISTICS OF THE SYSTEM

11.1. INTRODUCTION

The first part of the report is devoted to the description of the system. The system is a control system for a process. The process is a second-order system with a time constant of 1 second and a natural frequency of 1 rad/sec. The system is controlled by a proportional controller. The transfer function of the system is given by

$$G(s) = \frac{K}{s^2 + 2s + 1}$$

where  $K$  is the gain of the controller. The system is controlled by a proportional controller with a gain of 1. The transfer function of the controller is given by

$$C(s) = K_c$$

The closed-loop transfer function of the system is given by

$$T(s) = \frac{K_c}{s^2 + 2s + 1 + K_c}$$

The system is controlled by a proportional controller with a gain of 1. The transfer function of the controller is given by

$$C(s) = 1$$

The closed-loop transfer function of the system is given by

$$T(s) = \frac{1}{s^2 + 2s + 2}$$

The system is controlled by a proportional controller with a gain of 1. The transfer function of the controller is given by

$$C(s) = 1$$

The closed-loop transfer function of the system is given by

$$T(s) = \frac{1}{s^2 + 2s + 2}$$

The system is controlled by a proportional controller with a gain of 1. The transfer function of the controller is given by

$$C(s) = 1$$

The closed-loop transfer function of the system is given by

$$T(s) = \frac{1}{s^2 + 2s + 2}$$

The system is controlled by a proportional controller with a gain of 1. The transfer function of the controller is given by

$$C(s) = 1$$

The closed-loop transfer function of the system is given by

$$T(s) = \frac{1}{s^2 + 2s + 2}$$

The system is controlled by a proportional controller with a gain of 1. The transfer function of the controller is given by

$$C(s) = 1$$

The closed-loop transfer function of the system is given by

$$T(s) = \frac{1}{s^2 + 2s + 2}$$

The system is controlled by a proportional controller with a gain of 1. The transfer function of the controller is given by

$$C(s) = 1$$

The closed-loop transfer function of the system is given by

$$T(s) = \frac{1}{s^2 + 2s + 2}$$

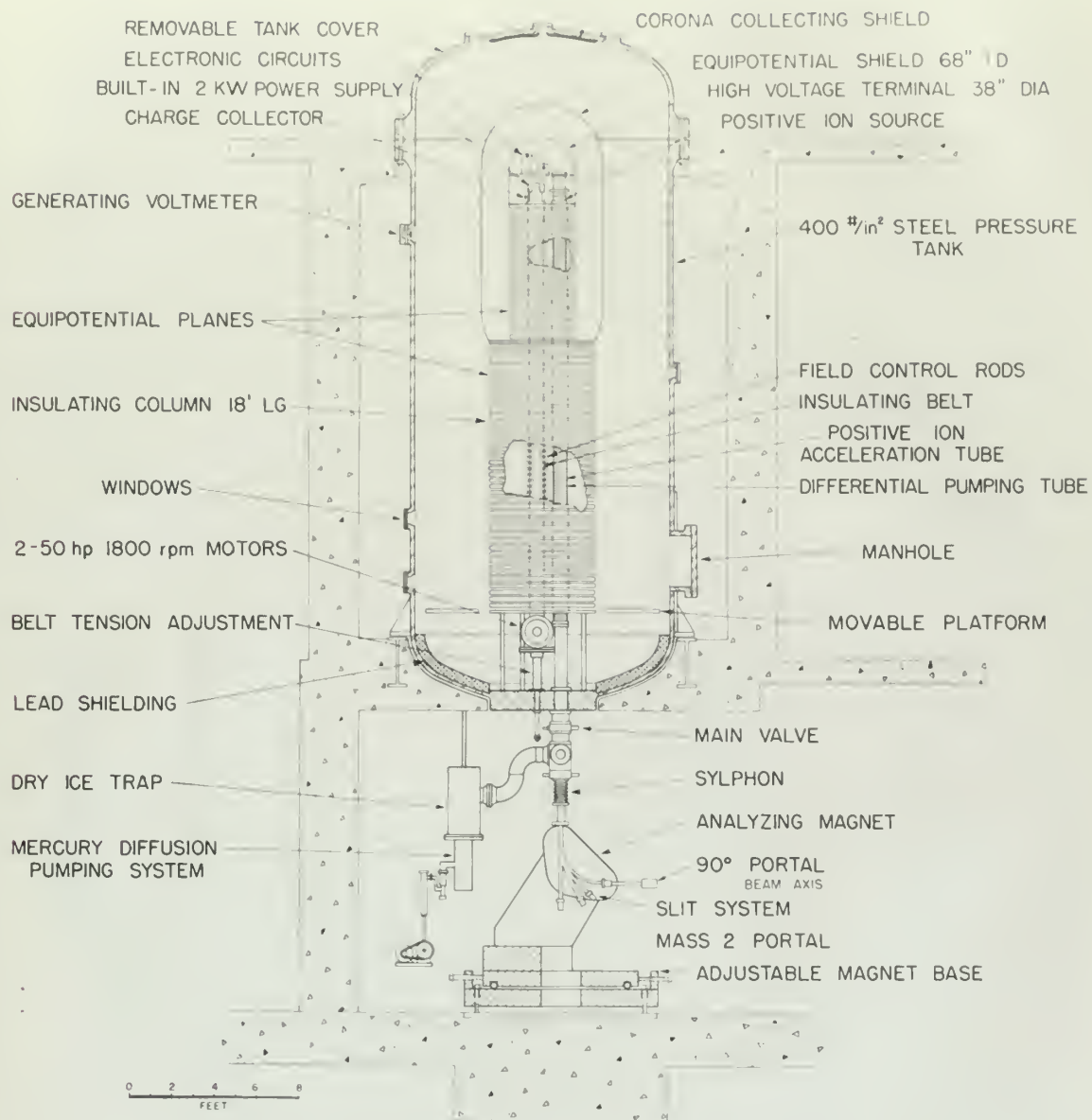
The system is controlled by a proportional controller with a gain of 1. The transfer function of the controller is given by

$$C(s) = 1$$

The closed-loop transfer function of the system is given by

$$T(s) = \frac{1}{s^2 + 2s + 2}$$





12 MEV POSITIVE ION ACCELERATOR FOR M.I.T.

Figure 2





VAN DE GRAAFF GENERATOR  
ACCELERATING TUBE

MAGNETIC  
ANALYZER

CAMERA

180° MAGNETIC  
SPECTROGRAPH

TARGET CHAMBER

FLUXMETER  
OSCILLATOR

Figure 3

РОТАРНИЙ ПЛАТФОРМА  
УСКОРЕНИЕ

СИТНИК  
РЕЗУЛЬТАТ

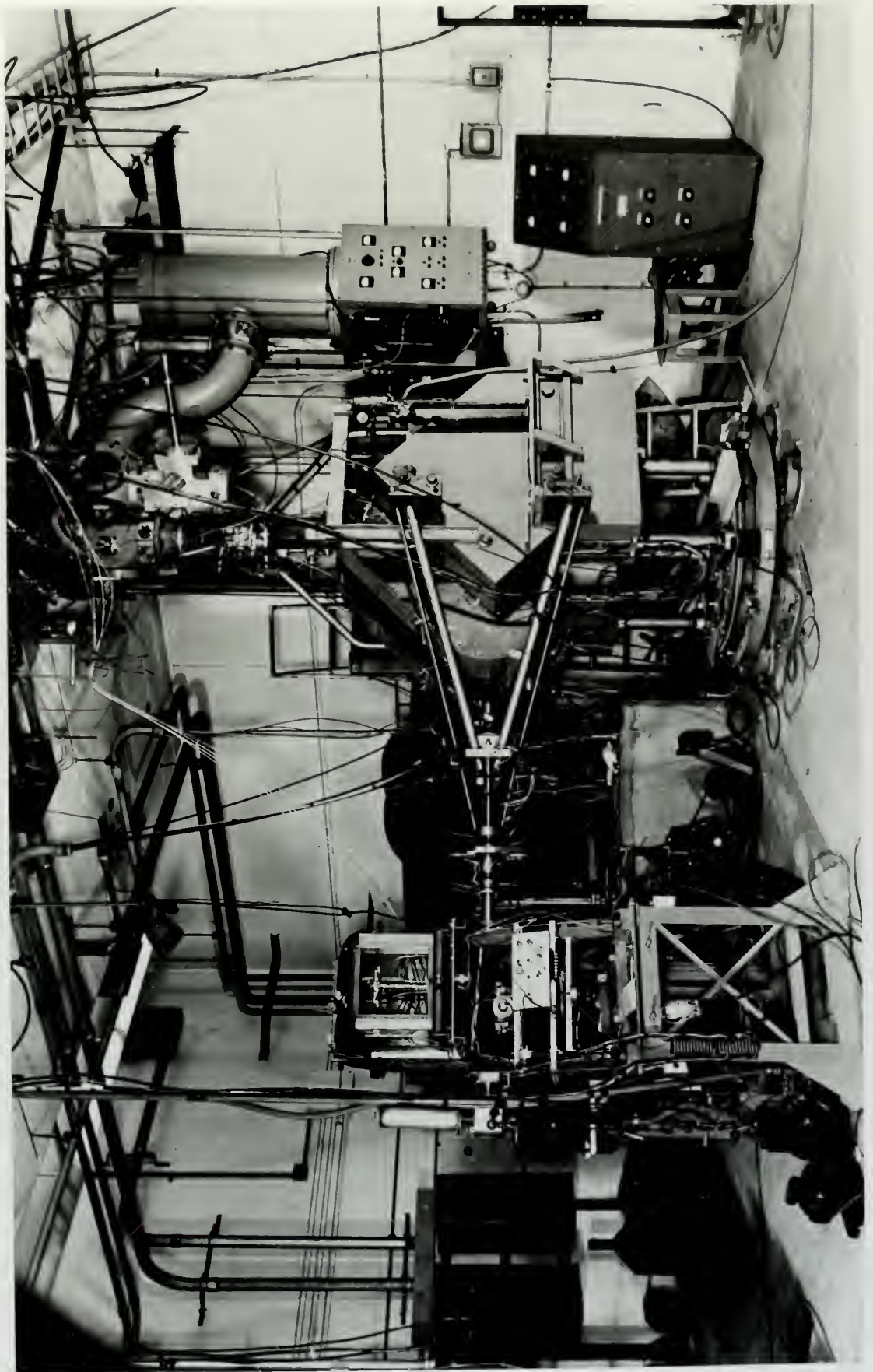
РЕЗОНАНСНАЯ КАМЕРА

РЕЗОНАНСНАЯ  
КАМЕРА

СИТНИК  
180°

КАМЕРА

Figure 3







to deflect particles either to a fixed,  $180^\circ$  focusing magnetic spectrograph, which observes reaction products only at  $90^\circ$  from the incident beam, or to the new rotatable spectrograph. Only the fixed magnet was used in this work.

The fixed magnetic spectrograph is fitted with entrance slits to define the beam position and energy, and a Faraday bucket arrangement for measuring beam current. The bottom of the annular magnet is slotted to accept the incident particles. A detailed account of this spectrograph is given by Strait.<sup>10</sup>

The charged particles from the nuclear reaction which emerge in the acceptance angle of the spectrograph are deflected with a radius proportional to their momentum and recorded on a 1" X 2" Eastman NTA nuclear track plate placed in a slot along the top of the magnet. These track plates are positioned with their long dimension vertical and with the normal to the emulsion at about  $70^\circ$  from the incident particles in a carriage which can hold, and position in turn, five such plates. A light, prism, and slit arrangement is available to "index" the plates at a fixed vertical position.

The magnetic fields in the analyzing and spectrographic magnets are determined by a nuclear resonance technique,

to define position relative to a fixed, 100° longitude meridian  
geographically, which however remains positive only as far  
from the center line, or to the non-rotatable geocentric  
only the fixed center was used in this case.

The fixed geocentric geocentric is fixed with respect  
also to define the base position and energy, and a further  
fixed arrangement for secondary base curves. The center  
of the center was it fixed to serve the latitude  
position. A detailed account of this geocentric is  
given in Table 10.

The change position from the center position which  
serves in the geocentric case of the geocentric case  
related with a certain proportion to the center and  
related on a 10° 20' distance with respect to the fixed  
in a line along the top of the segment. These lines  
are parallel with each other and parallel with the  
the center in the position of about 10° from the latitude  
position in a secondary case was fixed, and position in  
the, the same position. A further, the same position  
and in relation to the center the position of a fixed position  
position.

The position of the center and geocentric  
position was determined by a certain secondary position.

utilizing the known gyromagnetic ratio of the  $\text{Li}^7$  nucleus. Each magnet is equipped with a high frequency oscillator whose loading coil surrounds a capsule of a lithium salt solution placed in the field. In operation the oscillator is "zero-beated" with a secondary frequency standard and the current to the magnet is increased until the oscillator output is decreased, indicating resonance. Resonance is observed by sweeping the field in the vicinity of the capsule with a weak 60 cycle field and displaying the detected output of the oscillator on the vertical sweep of an oscilloscope which is swept in the horizontal direction with this same 60 cycle signal. When resonance is achieved the oscillator will be loaded twice a cycle with an angular displacement of  $180^\circ$ , and the two depressions on the scope face will be opposite each other. As the field current drifts from the correct value, the angular separation of the two depressions (loadings) will decrease, indicating that magnetic resonance is occurring only near the upper or lower variation of the sweep field. A phase control permits setting a variable phase between the 60 cycle sweep signal and the detected oscillator output, so that the two depressions may be superimposed. The magnet current is adjusted so that signals remain displaced by  $180^\circ$  as the sweep current is made vanishingly small. The error intro-







duced by virtue of the fact that the two depressions are not exactly  $180^\circ$  apart can best be estimated by varying the signals as a function of zero-beat frequency. When this is done it seems that the sensitivity of the visual signal is about .5 kc at a frequency of 19.0 mc. The zero-beat frequency itself, on a reasonably careful run, is kept below 1 kc, so that the reproducibility of the magnetic field at the capsule is in error by about one part in 20,000 (1:20,000).

The known gyro-magnetic ratio of the lithium nucleus is used to determine the magnetic field, assumed to be the effective field experienced by the charged particles. This assumption, which may be in error by perhaps .1%, leads to a very small error in measured moments, as is seen below. The diameter of the trajectory in the spectrograph from the target spot to the index is determined by use of a polonium-coated wire at the target position. The BR of polonium alphas is  $331.588 \pm .02\%$  kilogauss-cm.<sup>11</sup> The wire to beam spacing is measured with a microscope to  $\pm .05$  mm, and is very small compared to the diameter. The fractional error in magnetic field,  $dB/B$ , yields a fractional error,  $dR_a/R_a = -dB/B$  in the measured radius of the path from polonium wire to the alpha tracks on the emulsion, where  $R_a =$  radius of trajectory of alpha particles.

In measuring moments of charged particles from nuclear



reactions, the error introduced is then  $RdR - RdB = -dR R_0 - RdB = dB(-R_0 - R)$ , where  $R =$  radius of the trajectory of these particles. We have assumed that  $dB/B$  is constant and that  $dR_0 = dR$ .

The average radius is 35 cm and the useable portion of the emulsion is 3.5 cm, so that the maximum difference ( $R - R_0$ ) is .9 cm, or 2.5%. The total error due to non-uniformity of the magnetic field is then less than 1 part in 40,000. It is seen that a 0.1% error in the value of the magnetic moment of the lithium nucleus would lead to an equally negligible error. The validity of the assumption of a constant  $dB/B$  may be questioned at high fields (because of the air gaps and saturation) and this may account for a suspected decrease in accuracy for fields over 13 kilogauss.

#### B. TARGET PREPARATION

Thin targets, when bombarded by charged particles, yield the advantage of a sharp group of reaction products, inasmuch as the degradation of the energy of the incident particles is slight. A common method of preparing thin metallic targets is by the evaporation in a high vacuum of the desired metal onto a thin ( $\sim 1000\mu$ ) Formvar film. This method becomes difficult with high boiling point metals, and in spite of the adoption of the method used by Schwager and



The first part of the paper is devoted to a general discussion of the problem. It is shown that the problem is well-posed in the sense of Hadamard. The second part is devoted to the construction of the solution. It is shown that the solution exists and is unique. The third part is devoted to the numerical solution of the problem. It is shown that the numerical solution is stable and accurate. The fourth part is devoted to the application of the results to the problem of the stability of the system. It is shown that the system is stable.

The first part of the paper is devoted to a general discussion of the problem. It is shown that the problem is well-posed in the sense of Hadamard. The second part is devoted to the construction of the solution. It is shown that the solution exists and is unique. The third part is devoted to the numerical solution of the problem. It is shown that the numerical solution is stable and accurate. The fourth part is devoted to the application of the results to the problem of the stability of the system. It is shown that the system is stable.

The first part of the paper is devoted to a general discussion of the problem. It is shown that the problem is well-posed in the sense of Hadamard. The second part is devoted to the construction of the solution. It is shown that the solution exists and is unique. The third part is devoted to the numerical solution of the problem. It is shown that the numerical solution is stable and accurate. The fourth part is devoted to the application of the results to the problem of the stability of the system. It is shown that the system is stable.

Cox<sup>12</sup> to evaporate vanadium, only a limited success was realized with cobalt. The extreme boiling temperature (approximately 3000°C) caused all those Formvar backings which survived to be extremely brittle, and the explosive nature of the boiling riddled the targets with small holes. Coating the reverse side of the Formvar with gold did not help to any extent. The maximum thickness of cobalt successfully evaporated in this fashion was something less than one-half that required to make a microscope slide opaque to sunlight. These targets, when exposed to deuteron beams of reasonably long exposures, yielded proton groups too weak to reduce the statistical fluctuations to an acceptable value. Recourse was then had to acceptable platinum backed targets. A sheet of platinum about 5 mils thick was carefully cleaned with hydrochloric acid and exposed in a vacuum to vaporized cobalt. Two one-fourth inch carbon electrodes were mounted vertically, with the lower rod hollowed out to hold a small piece of cobalt and necked down immediately below to perhaps one-tenth its original area, and the upper rod sharpened to a dull point and pressed down on the cobalt. The platinum was placed much closer than the Formvar had been, and a coating equal to that which was just greater than opaque to sunlight on a microscopic slide was achieved after several evaporations. It may be wondered whether the



The first part of the report is devoted to a general survey of the  
 progress of the work during the year. It is followed by a detailed  
 account of the various experiments conducted, and the results  
 obtained. The second part of the report is devoted to a  
 discussion of the theoretical principles which govern the  
 phenomena observed, and to a comparison of the experimental  
 results with the theoretical predictions. The third part of  
 the report is devoted to a summary of the work done during  
 the year, and to a list of the publications which have  
 resulted from the work. The fourth part of the report is  
 devoted to a list of the names of the persons who have  
 assisted in the work, and to a list of the names of the  
 persons who have been consulted in connection with the  
 work. The fifth part of the report is devoted to a list of  
 the names of the persons who have been consulted in  
 connection with the work. The sixth part of the report is  
 devoted to a list of the names of the persons who have  
 been consulted in connection with the work. The seventh part  
 of the report is devoted to a list of the names of the  
 persons who have been consulted in connection with the work.

sputtering which previously pierced the Formvar did not spatter the platinum in a random fashion, and such may indeed have been the case, although no evidence of this was seen in the results.

These targets were fixed to small rods and, for bombardment, mounted on a target wheel located just below the slot in the spectrographic magnet. Seven such targets could be mounted on the wheel and any one could then be rotated into the beam without breaking the vacuum. The targets were placed so that their normals were at approximately  $50^\circ$  to the incident beam and  $40^\circ$  to the annular chamber. When solid targets were used, the beam current integrator, developed by Enge,<sup>13</sup> was connected to the target wheel rather than to the Faraday bucket.



### III. EXPERIMENTAL PROCEDURE

In the process of identifying and measuring the proton groups from cobalt, the first step was to bombard a Formvar-backed target with protons and analyze the elastically scattered proton groups for the mass of the scattering nuclei in order to determine the contaminants. For scattering at  $90^\circ$  from a target initially at rest, we get, non-relativistically,

$$n = \frac{E_{in}m_p + E_o m_p}{E_{in} - E_o}, \quad \text{where } m_p = \text{proton mass.}$$

$E_o$ , the energy out, is measured by recording the density of proton tracks per one-half mm (measured radially) along the nuclear track plate, to within .04 mm as the plate is traversed in a vernier-calibrated microscope stage. Protons, deuterons, and alpha tracks can be distinguished by their length and density of ionization. The index is recorded to the nearest .02 mm. The points then obtained are graphed, a curve is faired through them, and the position of the third height is noted. This position has been found to give the most reproducible results, regardless of peak intensity or target thickness, and the index to third height differences, when measured with different microscopes, have been found to have a probable error of about .15 mm. This distance is then subtracted from the index to beam distance, as measured by the



## III. EXPERIMENTAL PROCEDURE

In the process of identifying and separating the proton groups from acetate, the first step was to measure a proton-  
 related signal with respect to the standard  
 standard proton group for the sake of the standard  
 signal in order to determine the distribution. For separating  
 we use a proton signal of acetate, for exam-

plification,

$$R = \frac{A_1 + A_2}{A_1 - A_2} \quad \text{where } A = \text{proton mass.}$$

$A_1$ , the heavy one, is a measure of resonating the quality  
 of proton signals for acetate as (proton) velocity along  
 the nuclear spin plane, as shown. As an example is  
 traversed in a vertical-tilted cylindrical pipe. Protons,  
 distributed, and also those can be distinguished by their  
 length and density of radiation. The beam is scattered to  
 the center of the pipe. The points that obtained are grouped,  
 a curve is traced through them, and the position of the third  
 height is noted. This position has been found to give the  
 most reproducible results, regardless of proton intensity or  
 target thickness, and the same to third height differences,  
 when measured with different equipment, have been found to  
 have a probable error of about 1.5%. This distance is then  
 subtracted from the total to local distance, as measured by the



polonium alphas, and the result halved to get the radius. The magnetic field is taken as a fixed constant multiplied by the frequency of the oscillator and, as seen before, this should introduce no significant error. The product of radius and magnetic field, BR, is then converted to proton energy by means of an extensive table calculated from

$$E_p = 4.7898 \times 10^{-11} (BR)^2 - 1.223 \times 10^{-24} (BR)^4$$

$E_{in}$ , the energy in, is determined from elastically scattered particles from a known mass such as Co<sup>59</sup>, or O<sup>16</sup>. Figure 4 presents a graphic mass analysis, with the most probable contaminants indicated.

The first known excited state<sup>8</sup> of Co<sup>59</sup> is 1.10 Mev, from which level the inelastic protons would have insufficient energy to appear in Figure 4. Those mass numbers between 48 and 80 are not separated from the Co<sup>59</sup> peak. It is seen that Na<sup>23</sup>, Mg<sup>24</sup>, S<sup>32</sup>, Cl<sup>35</sup> and K<sup>39</sup> are present. A spectrochemical analysis of the cobalt pellets indicated the following contaminants:

Ni:	10% to .1%
Mg and Cu:	1% to .01%
Ca, Fe, and Mn:	.1% to .001%
Ag, Al, B, Ba, Cr, Si, and Zn:	less than .01%

The sodium, potassium, and sulphur, seen in the mass analysis of a Formvar target, probably originate in the Formvar

... and the ... of the ...  
 ... is ... in the ...  
 ... of the ... and, ...  
 ... in ... The ...  
 ... is ... to ...

$$E = \frac{1}{2}mv^2 = \frac{1}{2}m\omega^2 r^2 = \frac{1}{2}m\omega^2 \left(\frac{h}{m\omega}\right)^2 = \frac{1}{2} \frac{h^2 \omega^2}{m}$$

... the ... is ...  
 ... from ...  
 ... with the ...  
 ...

... of ...  
 ... the ...  
 ... in ...  
 ... from ...  
 ...

... of the ...  
 ...

...	...
...	...
...	...
...	...

... in the ...  
 ... of a ...

ELASTIC PROTONS FROM  
FORMVAR TARGET.  $E_p = 5.2 \text{ Mev}$

Mass numbers of contaminants  
are as indicated.

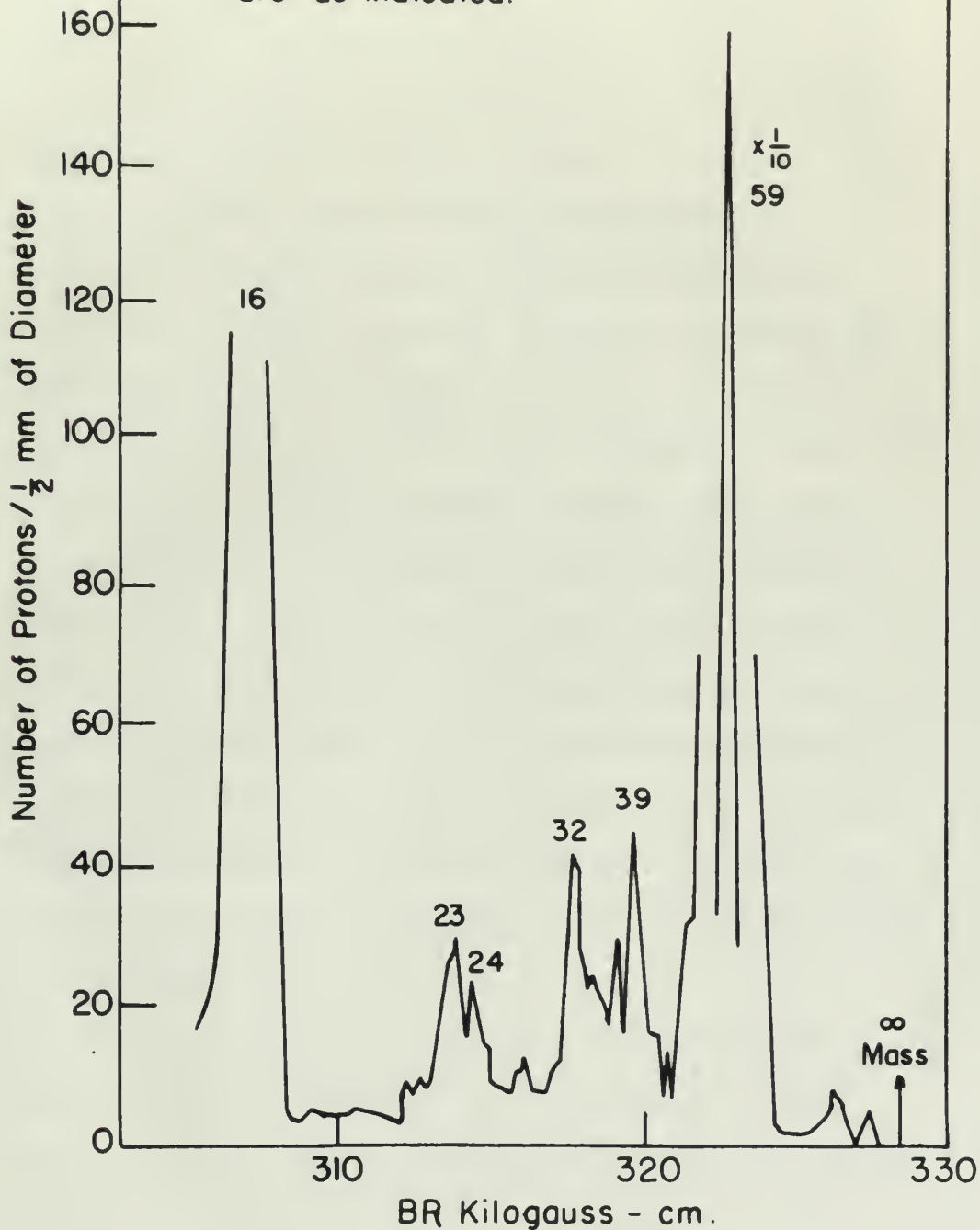


Figure 4





backing, and hence should not contribute proton groups in the bombardment of the platinum-backed targets. Groups from the platinum itself, if present, should be very broad, because of the thickness of the backing.

Formvar targets coated with cobalt were then bombarded with 5.0 Mev deuterons and the resultant proton groups were plotted. At each current setting of the spectrograph, the target was exposed to from 150 to 400 microcoulombs of deuterons, requiring from one to four hours per plate. The spectrograph field was changed in steps so as to cover an appreciable range of momentum, with the steps so arranged that the graphs from adjacent plates overlapped. With each set of plates at least one elastic was taken to calibrate the input energy. The ground and metastable states and some excited states were evident, but the yield was so low (a maximum of 36 counts per  $1/2$  mm for the ground state, for example,) that the statistics were poor, and weak peaks were entirely obscured. This was repeated for a portion of the spectrum with a bombarding energy of 5.8 Mev, but the results were no better.

Next the platinum-backed targets were bombarded at energies of 5.0 and 5.8 Mev. The input energy for each set of plates was again determined with at least one elastic group from a Formvar target and each exposure was of 600



The first part of the paper is devoted to a study of the
 properties of the  $\beta$ -rays emitted in the decay of
  $^{137}\text{Ba}$ . The energy spectrum of the  $\beta$ -rays was
 measured with a Geiger-Müller tube and a scaler.
 The results are shown in Figure 1. The spectrum
 consists of a continuous part and a sharp peak at
 0.54 Mev. The continuous part is due to the
 decay of  $^{137}\text{Ba}$  into  $^{137}\text{La}$  and the sharp
 peak is due to the decay of  $^{137}\text{Ba}$  into
  $^{137}\text{La}$  and  $\gamma$ -rays. The energy of the
  $\gamma$ -rays was measured with a NaI(Tl) crystal
 and a scaler. The results are shown in Figure
 2. The spectrum consists of a sharp peak at
 0.66 Mev. The energy of the  $\gamma$ -rays is
 0.66 Mev. The results are in good agreement
 with the values given in the literature.

The second part of the paper is devoted to a study
 of the properties of the  $\beta$ -rays emitted in the
 decay of  $^{137}\text{Ba}$ . The energy spectrum of the
  $\beta$ -rays was measured with a Geiger-Müller tube
 and a scaler. The results are shown in Figure
 3. The spectrum consists of a continuous part
 and a sharp peak at 0.54 Mev. The continuous
 part is due to the decay of  $^{137}\text{Ba}$  into
  $^{137}\text{La}$  and the sharp peak is due to the
 decay of  $^{137}\text{Ba}$  into  $^{137}\text{La}$  and  $\gamma$ -rays.
 The energy of the  $\gamma$ -rays was measured with
 a NaI(Tl) crystal and a scaler. The results
 are shown in Figure 4. The spectrum consists
 of a sharp peak at 0.66 Mev. The energy of
 the  $\gamma$ -rays is 0.66 Mev. The results are
 in good agreement with the values given in
 the literature.

microcoulombs duration. Because of the intense deuteron background from single and multiple scattering from the platinum backing, it was necessary to cover the plates with aluminum foil of sufficient thickness to stop the deuterons. The result of the plot of protons versus BR, covering the ground and first excited states, is shown in Figure 5. A typical plate at higher excitation showing the increase in density of levels, is shown in Figure 6. Figure 7 is a plot of the proton groups from the ground state to an excitation of 4.8 Mev with  $E_{in}$ , the deuteron bombarding energy, equal to 5.0 Mev.

In computing the momentum of a group of particles, the peak is replotted with abscissa expanded by a factor of 20.

A sample calculation, taken from plate 2IV follows:

Abscissa of index	11.040 cm
Minus abscissa of 1/3 height of peak	<u>9.537</u>
	Δ 1.503 cm
Measured beam to index distance	71.757 cm
	Δ <u>1.503</u>
Diameter of proton trajectory	70.254 cm

$$\text{Radius of proton trajectory} = \frac{70.254}{2} = 35.127 \text{ cm.}$$



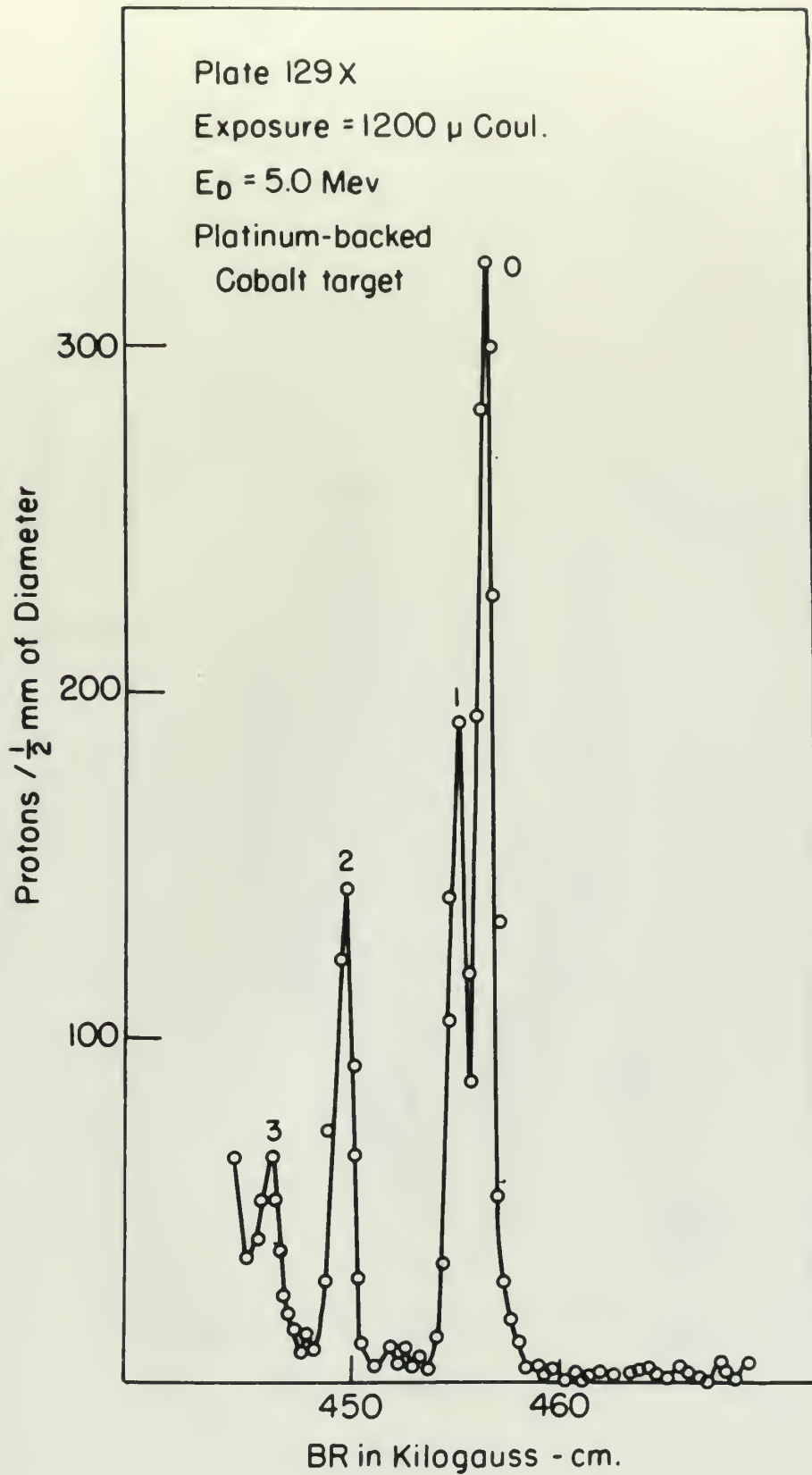


Figure 5





Plate 134 X

Exposure  $\approx 600 \mu$  Coul.

$E_D \approx 5.0$  Mev

Platinum-backed Cobalt target

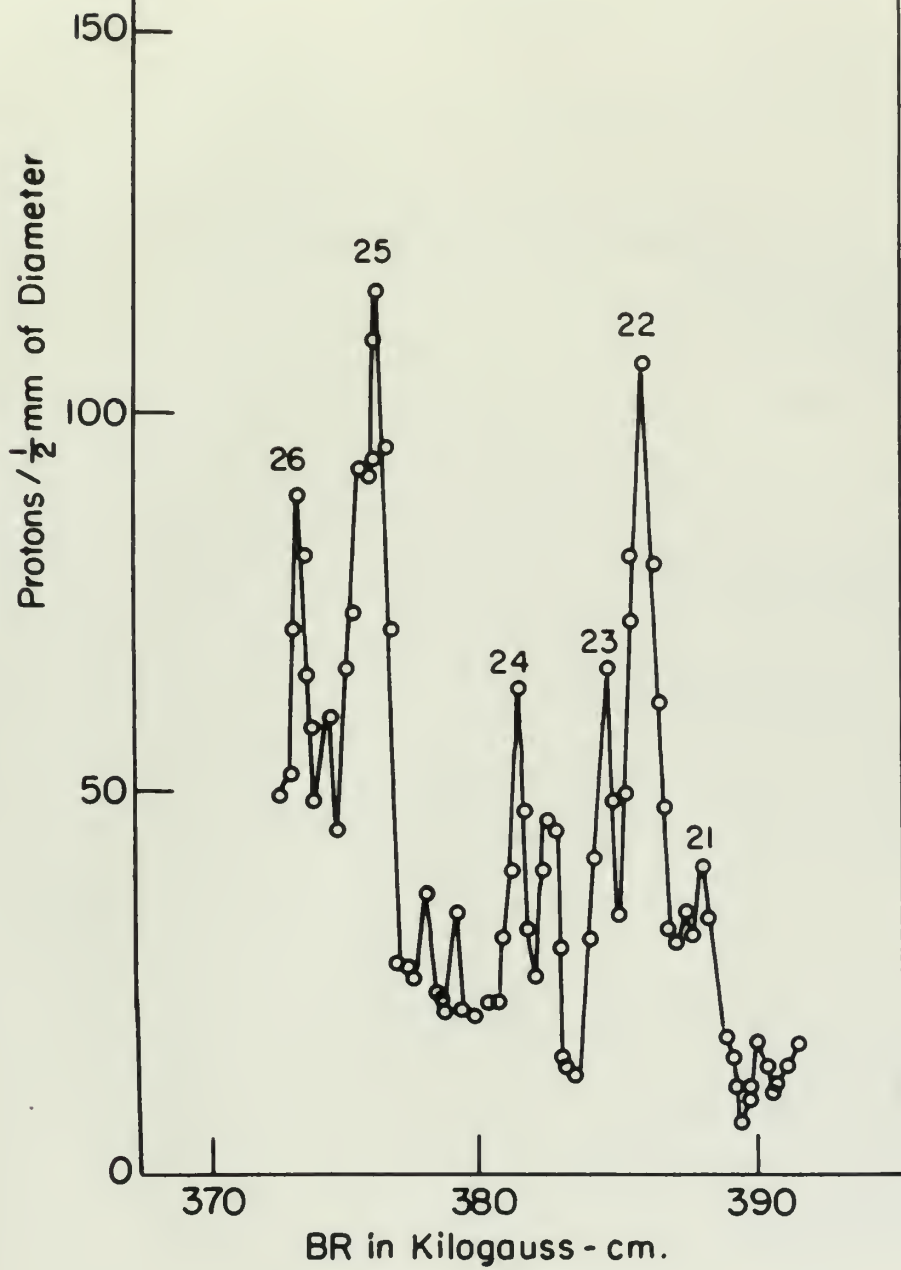


Figure 6



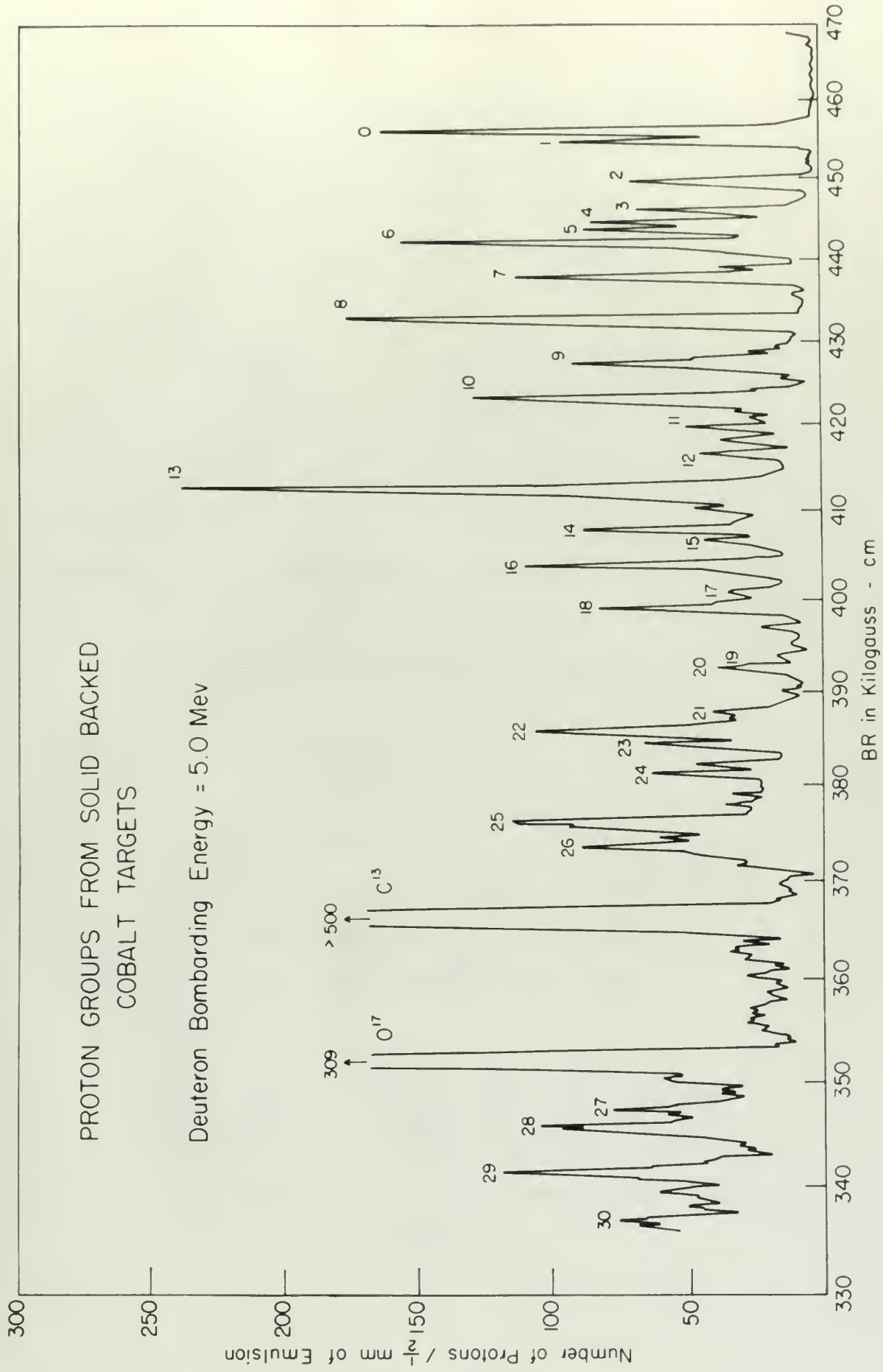


Figure 7



Frequency of spectrographic magnet fluxmeter = 21.300 mc.

$$B = \frac{21.300 \text{ mc}}{1.6545 \text{ mc/kg}} = 12.873 \text{ kilogauss}$$

$$BR = 12.873 \times 35.127 = 452.197 \text{ kilogauss-cm.}$$

From BR tables

$$E_0 = 9.73470 \quad (\text{BR} = 452 \text{ kilogauss-cm})$$

$$\frac{845}{9.74315} \quad (\text{interpolation})$$

$$9.74315 \quad \text{MeV}$$

$$E_{1n} = 5.824$$

$$Q = \frac{(M_T - M_0)}{M_T} E_0 - \frac{(M_T - M_1)}{M_T} E_1 =$$

$$1.10168 \times 9.7432 - 0.96640 \times 5.8240 = 4.2785 \text{ MeV}$$

where  $M_T = \text{Co}^{60} = 59.9364 \text{ amu}$

$$M_0 = p = 1.00759 \text{ amu}$$

$$M_1 = d = 2.01419 \text{ amu.}$$

Relativistic correction = +1.1 kev. This relativistic correction came about by virtue of the fact that the Q-equation was derived for the nonrelativistic case.

The equation is

$$dQ = E_{1n}^2 \frac{M_T^2 - M_1^2}{1842 M_T^3} + E_0^2 \frac{M_T^2 - M_0^2}{1842 M_T^3} - E_{1n} E_0 \frac{M_1 M_0}{931 M_T^3}$$

$$Q + dQ = 4.2796 \text{ MeV.}$$



Forming of ...

$$y = \frac{11.000 \text{ m}}{1.000 \text{ m}} = 11.000$$

$$m = 11.000 \times 10.000 = 110.000$$

From the table

$$c_0 = 0.0000$$

$$\frac{dy}{dx}$$

$$0.0000$$

$$2.000 = 2.000$$

$$y = \frac{11.000 - 0.000}{1.000} = 11.000$$

$$1.000 \times 0.000 = 0.000$$

$$c_0 = 0.000 = 0.000$$

$$c_1 = 0 = 0.000$$

$$c_2 = 0 = 0.000$$

... ..

... ..

... ..

The equation is

$$y = \frac{11.000 - 0.000}{1.000} = 11.000$$

$$y = 11.000$$

Finally, runs were made at 3.0 Mev to attempt to uncover the region obscured at 5.0 Mev by the intense carbon and oxygen peaks, and to repeat the measurement of the ground state Q-value. This was accomplished by holding the generator at 6 Mev and deflecting singly charged deuterium molecules. In a nuclear reaction the chemical binding energy of the molecule is negligible, each nucleus taking half the energy. The coulomb barrier, which is 6.6 Mev for compound nucleus formation, must have effectively reduced the (d,p) reaction probability at the energy, however, as only a negligible yield resulted.

In analyzing the results there are three ways to identify the residual nucleus of a reaction group. The first is to vary the composition of the target and note the corresponding variations in peak intensities. This was not intentionally done. The second is to match peaks with previously determined Q-value of known contaminants, and the third is by means of an energy shift. It is seen from the formula for  $E_0$ ,

$$E_0 = \frac{M_T - M_1}{M_T + M_0} E_1 + \frac{M_T}{M_T + M_0} Q, \text{ where } M_T \text{ is the mass of}$$

the residual nucleus, that the energy (and hence momentum) of a peak is a function of  $M_T$ . The output energy of a group

The first part of the paper is devoted to a study of the  
 properties of the function  $f(x)$  which is defined by the  
 equation  $f(x) = \int_0^x f(t) dt$ . It is shown that  $f(x)$  is  
 a constant function and that the only solution of the  
 equation  $f(x) = \int_0^x f(t) dt$  is  $f(x) = 0$ . The  
 second part of the paper is devoted to a study of the  
 properties of the function  $g(x)$  which is defined by the  
 equation  $g(x) = \int_0^x g(t) dt + x$ . It is shown that  
 $g(x)$  is a linear function and that the only solution  
 of the equation  $g(x) = \int_0^x g(t) dt + x$  is  
 $g(x) = x$ .

The third part of the paper is devoted to a study of  
 the properties of the function  $h(x)$  which is defined  
 by the equation  $h(x) = \int_0^x h(t) dt + x^2$ . It is  
 shown that  $h(x)$  is a quadratic function and that  
 the only solution of the equation  $h(x) = \int_0^x h(t) dt + x^2$   
 is  $h(x) = x^2$ .

The fourth part of the paper is devoted to a study of  
 the properties of the function  $k(x)$  which is defined  
 by the equation  $k(x) = \int_0^x k(t) dt + x^3$ . It is  
 shown that  $k(x)$  is a cubic function and that the  
 only solution of the equation  $k(x) = \int_0^x k(t) dt + x^3$   
 is  $k(x) = x^3$ .

from  $\text{Ca}^{41}$ , for example, will shift 18 kev less per .8 Mev shift in input energy than that of a group from  $\text{Co}^{60}$ .

Similarly a group from  $\text{Br}^{80}$  will shift 10 kev more per .8 Mev shift in  $E_{in}$ .

The known groups from carbon and oxygen were identified. A small peak between groups 10 and 11 at 5.0 Mev bombarding energy which was not reproduced at 5.8 Mev matches a known  $\text{Mg}^{24}(d,p)$  group to within experimental error. Other known magnesium groups can be fitted, but not uniquely. The first excited level of  $\text{Ni}^{59}$ , seen in Kinsey's  $(n, \gamma)$  work, should lie just above the ground state of  $\text{Co}^{60}$  at a bombarding energy of 5.0 Mev, but was not seen. A structure on the low energy side of group 6 might be attributed to another group in Ni. All other groups of at least 50 counts per 1/2 mm of diameter yielded Q-values agreeing at the two input energies to within 12 kev when assigned to  $\text{Co}^{60}$ .

Above an excitation of 5 Mev, the proton background became large and widely variant between plates. This was thought to be due to a background of deuterons penetrating the foil by virtue of being deflected toward the normal to the foil. But it was shown that their range in the emulsion, even after passing through the foil at right angles,



The first part of the paper is devoted to the study of the
 asymptotic behavior of the eigenvalues of the operator
  $\Delta_{\epsilon}$  as  $\epsilon \rightarrow 0$ . It is shown that the eigenvalues
  $\lambda_{\epsilon}$  of  $\Delta_{\epsilon}$  are asymptotically equal to the eigenvalues
  $\lambda$  of the Laplacian  $\Delta$  on the manifold  $M$ .

In the second part of the paper, we study the asymptotic
 behavior of the eigenfunctions of  $\Delta_{\epsilon}$ . It is shown that
 the eigenfunctions  $\psi_{\epsilon}$  of  $\Delta_{\epsilon}$  are asymptotically
 equal to the eigenfunctions  $\psi$  of  $\Delta$  on  $M$ .

In the third part of the paper, we study the asymptotic
 behavior of the heat kernel of  $\Delta_{\epsilon}$ . It is shown that
 the heat kernel  $K_{\epsilon}(x, y, t)$  of  $\Delta_{\epsilon}$  is asymptotically
 equal to the heat kernel  $K(x, y, t)$  of  $\Delta$  on  $M$ .

In the fourth part of the paper, we study the asymptotic
 behavior of the spectral zeta function of  $\Delta_{\epsilon}$ . It is
 shown that the spectral zeta function  $\zeta_{\epsilon}(s)$  of  $\Delta_{\epsilon}$ 
 is asymptotically equal to the spectral zeta function  $\zeta(s)$ 
 of  $\Delta$  on  $M$ .

In the fifth part of the paper, we study the asymptotic
 behavior of the heat trace of  $\Delta_{\epsilon}$ . It is shown that
 the heat trace  $\text{Tr} e^{-t\Delta_{\epsilon}}$  of  $\Delta_{\epsilon}$  is asymptotically
 equal to the heat trace  $\text{Tr} e^{-t\Delta}$  of  $\Delta$  on  $M$ .



was vanishingly small, and increasing the thickness of the foil only blocked out all protons. These plates were further confused by the appearance of proton tracks of all lengths up to the maximum expected. The reason for this high background may be closely-spaced, overlapping levels in  $\text{Co}^{60}$ , or it may be from the platinum backing. Lack of time prevented a controlled run on a bare platinum target. In the course of the experiment about 64 plates were exposed.

The following is a list of the names of the persons who have been
 appointed to the various positions in the office of the
 Secretary of the Board of Education, for the year 1900-1901.
 The names are given in the order in which they were appointed.
 The names of the persons who have been appointed to the
 various positions in the office of the Secretary of the Board
 of Education, for the year 1900-1901, are given in the
 following list. The names are given in the order in which
 they were appointed.

## IV. RESULTS AND CONCLUSIONS

## A. PROBABLE ERROR.

An estimate of the probable error in Q-values is gotten by examining the system of measurements and assigning probable systematic and random errors.

The random errors considered are:

- (1) the spread in BR resulting from finite slit widths,
- (2) the spread in energy of emerging particles due to the variable thickness of cobalt the incident and reaction particles must penetrate,
- (3) the finite width of the beam,
- (4) the aberration of the  $180^\circ$  focusing magnet,
- (5) the finite "reaction" angle subtended by the photographic plate, and
- (6) small adjustments of the magnet currents necessary to keep the flux meter signal at the balanced position.

If one assumes an entrance slit width to the deflecting magnet of 1 mm, an exit slit width of 1 mm, and collimation of the entering and exit particles, one can make an order of magnitude estimate of the spread in BR of the analyzed particles



as  $dR/R = .5/600 = .0008$ . The energy loss in a thin, Forward-backed target is estimated as 10 kev, yielding a fractional spread in ER of .0005. The width of the line on the target was measured as 0.7 mm, or  $dR/R = .7/2 \times 350 = .001$ . The focusing action of the  $180^\circ$  magnet gives a fractional second order spread of the order of  $2(1 - \cos \theta) = 2 \theta^2/2$ .  $\theta$  is estimated as  $(2.5/2)/(35 \pi/2)$ , and  $dR/R = .0005$ . It has been estimated that<sup>11</sup> the plate subtends an angle of  $90^\circ \pm 1/3^\circ$  from the beam line on the target.

$$dE = 2 \sqrt{(M_1 M_0 E_1 E_0)} d \sin \theta / (M_0 + M_1), \text{ and}$$

$$dE/E = 2 \times 2 \left( \frac{1}{3} \pi / 180 \right) / 18 = .0013$$

for deuterons scattered from oxygen. This corresponds to  $dR/R = .0006$ . The two frequency settings each contribute errors of about 1:15,000, or  $dR/R = .00007$ . If we now take the square root of the sum of the squares of these estimated deviations and call this a gross approximation to  $\sigma$ , the standard deviation, we get  $\sigma (BR)/BR = 1.6 \times 10^{-3}$  as shown in Table I.

If the deuteron elastic of plate 22Y is fitted to a normal distribution,  $\sigma (BR)/BR = .065/70 = .9 \times 10^{-3}$ . This agreement is as good as could be expected, considering the approximations made. A similar value for  $\sigma (BR)$  is measured on well-developed cobalt (d,p) peaks.





## RANDOM ERRORS

Source	Magnitude of Error $\sigma$ (BR)/BR
Momentum spread of incident particles	.0008
Energy loss in cobalt	.0005
Width of line on target	.001
Aberration in 180° focusing magnet	.0005
Angle of observation	.0006
Deviations of B field	.0007
	$\sqrt{\sum \sigma_i / BR} = 1.6 \times 10^{-3}$

TABLE I

The following table shows the results of the survey conducted in  
 the year 1980. The data is presented in the following table.  
 The results are as follows:

To (1980)	From
1000	1000
2000	2000
3000	3000
4000	4000
5000	5000
6000	6000

$1000 \times 1.1 = 1100$

We do not actually have a Gaussian distribution, and it is the leading edge, not the mean, in which we are interested. If, nevertheless, we estimate the probable error as  $.67 \sigma / \sqrt{n}$ , where  $n \approx 250$  counts/peak, we get a random error of  $.67 \times .9 \times 10^{-3} / 16 = 1.25,000$ . This is about the precision to which the position of the leading edge is recorded.

The systematic errors are more important and harder to estimate. These include:

- (1) the calibration error of the polonium alpha groups,
- (2) the departure of the average scattering angle from  $90^\circ$ ,
- (3) surface films on the platinum- and Formvar-backed targets,
- (4) the uncertainty in the momentum of the polonium alphas,
- (5) the error in recording index to emulsion track distance in a given microscope, due to a cant of the plate in the microscope,
- (6) errors in the masses of the nuclei involved, and
- (7) errors in the fundamental constants,  $e$  and  $c$ .

The first part of the paper is devoted to a study of the error of the method of least squares. It is shown that the error of the method of least squares is of the order of  $\sqrt{n}$  where  $n$  is the number of observations. The error of the method of least squares is also compared with the error of the method of moments. It is shown that the error of the method of least squares is smaller than the error of the method of moments when the observations are normally distributed.

- to obtain. These results are
- (1) the relative error of the method of least squares is of the order of  $\sqrt{n}$  where  $n$  is the number of observations.
  - (2) the error of the method of least squares is smaller than the error of the method of moments when the observations are normally distributed.
  - (3) the error of the method of least squares is smaller than the error of the method of moments when the observations are normally distributed and the number of observations is large.
  - (4) the error of the method of least squares is smaller than the error of the method of moments when the observations are normally distributed and the number of observations is large and the observations are uncorrelated.
  - (5) the error of the method of least squares is smaller than the error of the method of moments when the observations are normally distributed and the number of observations is large and the observations are uncorrelated and the observations are independent.
  - (6) the error of the method of least squares is smaller than the error of the method of moments when the observations are normally distributed and the number of observations is large and the observations are uncorrelated and the observations are independent and the observations are normally distributed.
  - (7) the error of the method of least squares is smaller than the error of the method of moments when the observations are normally distributed and the number of observations is large and the observations are uncorrelated and the observations are independent and the observations are normally distributed and the observations are normally distributed.



The beam to index distance, as determined from the positions of polonium alpha groups, is deduced from the average of several groups, each group having been averaged in several microscopes. Two such measurements were taken during the course of this experiment and the reproducibility, 1:27,000, may be taken as a measure of the error.

The departure of the scattering angle from  $90^\circ$  can, in principle, be measured by noting the energy of the elastics from two nuclides with a common bombarding energy, but surface films confuse the results unless widely different nuclides, such as gold and lithium, are used. A recent calibration of this type has not been made, but the general consistency of results in the laboratory leads to the belief that this angle is not greater than 20 minutes, which, as has been seen, leads to an error of about 6.5 kev in the calibration of 5 Mev deuterons from oxygen. In computing the  $Q$  of the ground state of  $\text{Co}^{60}$  this is balanced by a term

$$\frac{2}{60} (5,000 \times 10,000 \times 12)^{1/2} \sin \theta = 2 \text{ kev}$$

so that the probable error, taken as half the "limit of error", is 2 kev.

The surface film, which was due primarily to an accumulation of carbon on the face of the target, has been estimated in other experiments to be from 5 to 20 kev thick. This would presumably affect the long-bombarded platinum-backed targets

The first of these elements, is the fact that the  
 position of the system is such that it is not  
 in a state of equilibrium, but that it is  
 in a state of motion. This is the case with  
 the system in this experiment and the velocity is  
 not to be taken as a measure of the work.

The position of the system is such that it is  
 not in a state of equilibrium, but that it is  
 in a state of motion. This is the case with  
 the system in this experiment and the velocity is  
 not to be taken as a measure of the work.

$$v = \frac{1}{2} \sqrt{\frac{2g}{L}} \sqrt{L} = \frac{1}{2} \sqrt{2gL}$$

The velocity of the system is such that it is  
 not in a state of equilibrium, but that it is  
 in a state of motion. This is the case with  
 the system in this experiment and the velocity is  
 not to be taken as a measure of the work.

more than the short elastics from the Formvar targets. But in this case a positive correction would be applied to the  $E_0$  of the ground state  $\text{Co}^{59}(\text{d},\text{p})$  reaction, increasing the measured  $Q$ , whereas our  $Q$ -value is already 20 kev greater than that of Bartholomew and Kinsey. A probable error of 5 kev is arbitrarily adopted.

The uncertainty in momentum of the polonium alphas is 1:5,000, or 1:2,500 in energy. Experience indicates that the probable error in reading a plate once on a microscope is  $.15 \text{ mm}/700 \text{ mm} = 1:5,000$  in ER, or 1:2,500 in energy. Errors in nuclear masses and fundamental constants are negligible as compared with the above.

The total probable error in the determination of the ground state  $Q$ -value from one oxygen elastic and one (d,p) reaction is, then, the combination of the randomness of the two measurements, the counting error of the two measurements, the surface film error, the polonium calibration error, the polonium momentum error, and reaction angle error. A tabulation of these errors is shown in Table II. The most important errors are those of film thickness and counting uncertainty.



The first part of the paper is devoted to the study of the asymptotic behavior of the solutions of the system (1.1) as  $t \rightarrow \infty$ . It is shown that the solutions of (1.1) are bounded and tend to zero as  $t \rightarrow \infty$ . The second part of the paper is devoted to the study of the asymptotic behavior of the solutions of the system (1.2) as  $t \rightarrow \infty$ . It is shown that the solutions of (1.2) are bounded and tend to zero as  $t \rightarrow \infty$ .

The third part of the paper is devoted to the study of the asymptotic behavior of the solutions of the system (1.3) as  $t \rightarrow \infty$ . It is shown that the solutions of (1.3) are bounded and tend to zero as  $t \rightarrow \infty$ . The fourth part of the paper is devoted to the study of the asymptotic behavior of the solutions of the system (1.4) as  $t \rightarrow \infty$ . It is shown that the solutions of (1.4) are bounded and tend to zero as  $t \rightarrow \infty$ .

The fifth part of the paper is devoted to the study of the asymptotic behavior of the solutions of the system (1.5) as  $t \rightarrow \infty$ . It is shown that the solutions of (1.5) are bounded and tend to zero as  $t \rightarrow \infty$ . The sixth part of the paper is devoted to the study of the asymptotic behavior of the solutions of the system (1.6) as  $t \rightarrow \infty$ . It is shown that the solutions of (1.6) are bounded and tend to zero as  $t \rightarrow \infty$ .

The seventh part of the paper is devoted to the study of the asymptotic behavior of the solutions of the system (1.7) as  $t \rightarrow \infty$ . It is shown that the solutions of (1.7) are bounded and tend to zero as  $t \rightarrow \infty$ .

TABULATION OF PROBABLE ERRORS IN DETERMINATION  
OF Q-VALUE OF GROUND STATE

Source	Magnitude, dE (kev)
Random:	
Oxygen Elastic	± .04
Proton Group	± .16
Systematic:	
Counting error in elastic	± 2.0
Counting error in proton group	± 4.0
Surface film error	± 5.0
Polonium calibration error	± .38
Polonium alpha momentum error	± 2
Reaction angle error	± 2
$\sqrt{\sum (dE)^2} = 7.4 \text{ kev}$	

TABLE II





For less well-developed peaks the probable error is increased. The excitation energy errors for groups which are seen on the same plate as the ground state, or on an adjacent, overlapping plate, is much less than the Q-value error, approaching 1 kev at low excitation.

## B. RESULTS

Three long exposures were made to investigate the vicinity of the ground state of  $\text{Co}^{60}$ : one with a deuteron bombarding energy of 5.0 Mev against a Formvar-backed target, one with a bombarding energy of 5.0 Mev against a platinum-backed target, and the third with a bombarding energy of 5.8 Mev against the same solid-backed target. These three exposures resulted in Q-values for the ground state which were within eleven kev of agreement. The ground state Q-value determined in this work ( $Q_0 = 5.280 \pm 0.008$  Mev) corresponds to the arithmetic mean of the two extreme values, and the spread corresponds to a laboratory nonreproducibility of about  $\pm 6$  kev. The third value resulted from bombardment of the thinly coated Formvar target and was of lower yield and poorer definition than the two others. All three exposures, however, clearly showed the separation of the 60 kev metastable state; and the computed excitations of this level, as well as the other listed levels, were unmistakably reproduced on both major series of bombardments (those against the platinum-backed targets).

The first experimental results are presented in Figure 1. The energy levels are shown as a function of the magnetic field. The energy levels are labeled as follows:  $E_1$ ,  $E_2$ ,  $E_3$ ,  $E_4$ ,  $E_5$ ,  $E_6$ ,  $E_7$ ,  $E_8$ ,  $E_9$ ,  $E_{10}$ ,  $E_{11}$ ,  $E_{12}$ ,  $E_{13}$ ,  $E_{14}$ ,  $E_{15}$ ,  $E_{16}$ ,  $E_{17}$ ,  $E_{18}$ ,  $E_{19}$ ,  $E_{20}$ ,  $E_{21}$ ,  $E_{22}$ ,  $E_{23}$ ,  $E_{24}$ ,  $E_{25}$ ,  $E_{26}$ ,  $E_{27}$ ,  $E_{28}$ ,  $E_{29}$ ,  $E_{30}$ ,  $E_{31}$ ,  $E_{32}$ ,  $E_{33}$ ,  $E_{34}$ ,  $E_{35}$ ,  $E_{36}$ ,  $E_{37}$ ,  $E_{38}$ ,  $E_{39}$ ,  $E_{40}$ ,  $E_{41}$ ,  $E_{42}$ ,  $E_{43}$ ,  $E_{44}$ ,  $E_{45}$ ,  $E_{46}$ ,  $E_{47}$ ,  $E_{48}$ ,  $E_{49}$ ,  $E_{50}$ ,  $E_{51}$ ,  $E_{52}$ ,  $E_{53}$ ,  $E_{54}$ ,  $E_{55}$ ,  $E_{56}$ ,  $E_{57}$ ,  $E_{58}$ ,  $E_{59}$ ,  $E_{60}$ ,  $E_{61}$ ,  $E_{62}$ ,  $E_{63}$ ,  $E_{64}$ ,  $E_{65}$ ,  $E_{66}$ ,  $E_{67}$ ,  $E_{68}$ ,  $E_{69}$ ,  $E_{70}$ ,  $E_{71}$ ,  $E_{72}$ ,  $E_{73}$ ,  $E_{74}$ ,  $E_{75}$ ,  $E_{76}$ ,  $E_{77}$ ,  $E_{78}$ ,  $E_{79}$ ,  $E_{80}$ ,  $E_{81}$ ,  $E_{82}$ ,  $E_{83}$ ,  $E_{84}$ ,  $E_{85}$ ,  $E_{86}$ ,  $E_{87}$ ,  $E_{88}$ ,  $E_{89}$ ,  $E_{90}$ ,  $E_{91}$ ,  $E_{92}$ ,  $E_{93}$ ,  $E_{94}$ ,  $E_{95}$ ,  $E_{96}$ ,  $E_{97}$ ,  $E_{98}$ ,  $E_{99}$ ,  $E_{100}$ .

### 3. RESULTS

The first experimental results are presented in Figure 1. The energy levels are shown as a function of the magnetic field. The energy levels are labeled as follows:  $E_1$ ,  $E_2$ ,  $E_3$ ,  $E_4$ ,  $E_5$ ,  $E_6$ ,  $E_7$ ,  $E_8$ ,  $E_9$ ,  $E_{10}$ ,  $E_{11}$ ,  $E_{12}$ ,  $E_{13}$ ,  $E_{14}$ ,  $E_{15}$ ,  $E_{16}$ ,  $E_{17}$ ,  $E_{18}$ ,  $E_{19}$ ,  $E_{20}$ ,  $E_{21}$ ,  $E_{22}$ ,  $E_{23}$ ,  $E_{24}$ ,  $E_{25}$ ,  $E_{26}$ ,  $E_{27}$ ,  $E_{28}$ ,  $E_{29}$ ,  $E_{30}$ ,  $E_{31}$ ,  $E_{32}$ ,  $E_{33}$ ,  $E_{34}$ ,  $E_{35}$ ,  $E_{36}$ ,  $E_{37}$ ,  $E_{38}$ ,  $E_{39}$ ,  $E_{40}$ ,  $E_{41}$ ,  $E_{42}$ ,  $E_{43}$ ,  $E_{44}$ ,  $E_{45}$ ,  $E_{46}$ ,  $E_{47}$ ,  $E_{48}$ ,  $E_{49}$ ,  $E_{50}$ ,  $E_{51}$ ,  $E_{52}$ ,  $E_{53}$ ,  $E_{54}$ ,  $E_{55}$ ,  $E_{56}$ ,  $E_{57}$ ,  $E_{58}$ ,  $E_{59}$ ,  $E_{60}$ ,  $E_{61}$ ,  $E_{62}$ ,  $E_{63}$ ,  $E_{64}$ ,  $E_{65}$ ,  $E_{66}$ ,  $E_{67}$ ,  $E_{68}$ ,  $E_{69}$ ,  $E_{70}$ ,  $E_{71}$ ,  $E_{72}$ ,  $E_{73}$ ,  $E_{74}$ ,  $E_{75}$ ,  $E_{76}$ ,  $E_{77}$ ,  $E_{78}$ ,  $E_{79}$ ,  $E_{80}$ ,  $E_{81}$ ,  $E_{82}$ ,  $E_{83}$ ,  $E_{84}$ ,  $E_{85}$ ,  $E_{86}$ ,  $E_{87}$ ,  $E_{88}$ ,  $E_{89}$ ,  $E_{90}$ ,  $E_{91}$ ,  $E_{92}$ ,  $E_{93}$ ,  $E_{94}$ ,  $E_{95}$ ,  $E_{96}$ ,  $E_{97}$ ,  $E_{98}$ ,  $E_{99}$ ,  $E_{100}$ .



In each of the two major series of investigations (at  $E_{in} = 5.0$  Mev and at  $E_{in} = 5.8$  Mev), good agreement resulted for the relative positions of the lower states in comparison with the respective ground states. The first eleven states in each of the series agreed to within five kev of each other. These lower states were seen under conditions which remained unchanged within each series, but which were different for each of the two series. The exceptionally good agreement in excited states which resulted led to the use of the average of each of these excited states in determining the Q-values of these levels. These Q-values, then, are the difference of the average ground state Q-value, which was determined less accurately, and the precise excitation energies. For the higher excited states, there being no simple correspondence in excitation energies, the Q-values of each level were determined by averaging the Q-values determined at each bombarding energy. Also, at these higher excitations, the increased number of weak levels arising from both contaminants and  $Co^{60}$  itself made resolution of the major peaks difficult. All levels attributed to  $Co^{60}$ , however, were in agreement to within 12 kev. In some instances it was possible to resolve a complex peak such that, by subtracting a minor peak, agreement was attained with the corresponding peak as determined at a different bombarding energy. This





technique was used only when it seemed justified by an obviously smaller structure indicated on a major peak.

Table III is a summary of the  $Q$ -values, excitation energies, appropriate probable errors, and approximate relative yields of those attributed to energy levels in  $\text{Co}^{60}$ .

#### C. COMPARISON WITH PREVIOUS RESULTS

The ground-state  $Q$ -value determined here,  $Q_0 = 5.280 \pm 0.008$  Mev, is in fair agreement with the values 5.20 determined by Bateson and Pollard<sup>6</sup>,  $5.44 \pm .2$  determined by Harvey<sup>1</sup>, and 5.31 determined by Hoesterey<sup>7</sup>. The more precise work of Bartholomew and Kinsey<sup>3</sup>, when the binding energy of the deuteron (2.226 Mev) is subtracted from their highest energy gamma-ray, results in a  $Q$  of  $5.260 \pm 0.006$ , a difference of 20 kev.

Table IV compares the excitation energies from this work with those found by Bartholomew and Kinsey and by Bateson and Pollard. It is seen that the excitation energies, particularly of the lower states are in excellent agreement. It is also of note that those low lying states of Bartholomew and Kinsey which stem from transitions indicated by strong homogeneous gamma-rays agree exceptionally well.

#### D. CONCLUSIONS

The metastable state in  $\text{Co}^{60}$  59 kev above the ground state is nicely brought out by the present work, and it is

... ..

... ..

... ..

... ..

... ..

... ..

... ..

... ..

... ..

... ..

... ..

... ..

... ..

... ..

... ..

... ..

... ..

... ..

... ..

... ..

... ..

... ..

... ..

## EXPERIMENTAL RESULTS

Peak	Q (MeV)	E <sup>+</sup> (MeV)	Relative Intensity
0	5.260 ± .008		1.0
1	5.220 ± .008	.060 ± .003	.6
2	4.994 ± .008	.286 ± .003	.5
3	4.835 ± .008	.445 ± .003	.4
4	4.767 ± .008	.513 ± .003	.5
5	4.723 ± .009	.557 ± .005	.5
6	4.659 ± .009	.621 ± .004	.9
7	4.488 ± .008	.792 ± .003	.7
8	4.268 ± .008	1.012 ± .003	1.0
9	4.043 ± .009	1.237 ± .005	.6
10	3.886 ± .009	1.394 ± .004	.8
11	3.747 ± .010	1.533 ± .006	.3
12	3.617 ± .010	1.663	.3
13	3.455 ± .010	1.825	1.5
14	3.278 ± .010	2.002	.5
15	3.219 ± .010	2.061	.7

TABLE III

TABLE I

Series	(mm) m	(mm) p	Age
0.1		100. ± 100.0	0
1.	100. ± 100.	100. ± 100.0	1
2.	100. ± 100.	100. ± 100.0	2
3.	100. ± 100.	100. ± 100.0	3
4.	100. ± 100.	100. ± 100.0	4
5.	100. ± 100.	100. ± 100.0	5
6.	100. ± 100.	100. ± 100.0	6
7.	100. ± 100.	100. ± 100.0	7
0.1	100. ± 100.1	100. ± 100.1	8
1.	100. ± 100.1	100. ± 100.1	9
2.	100. ± 100.1	100. ± 100.1	10
3.	100. ± 100.1	100. ± 100.1	11
4.	100. ± 100.1	100. ± 100.1	12
5.	100. ± 100.1	100. ± 100.1	13
6.	100. ± 100.1	100. ± 100.1	14
7.	100. ± 100.1	100. ± 100.1	15
8.	100. ± 100.1	100. ± 100.1	16
9.	100. ± 100.1	100. ± 100.1	17



## EXPERIMENTAL RESULTS

Peak	Q (MeV)	$E_{\beta}$ (MeV)	Relative Intensity
16	3.123 ± .010	2.154	.5
17	2.932 ± .010	2.792	.2
18	2.910 ± .015	2.370	.5
19	2.665 ± .010	2.615	.1
20	2.650 ± .010	2.630	.2
21	2.489 ± .012	2.791	.3
22	2.409 ± .015	2.871	.6
23	2.356 ± .012	2.924	.4
24	2.242 ± .012	3.038	.4
25	2.069 ± .012	3.211	.7
26	1.971 ± .012	3.309	.4
27	1.054 ± .012	4.226	.4
28	.974 ± .013	4.306	.6
29	.855 ± .012	4.425	.7
30	.709 ± .015	4.571	.5

TABLE III (Continued)



TABLE I

Wavelength (Å)	$\nu$ (cm <sup>-1</sup> )	$\epsilon$ (l/mole-cm)	Assignment
210	4762	1000 ± 500	ν(C=O)
220	4545	100 ± 50	ν(C=C)
230	4348	200 ± 100	ν(C=C)
240	4167	100 ± 50	ν(C=C)
250	4000	100 ± 50	ν(C=C)
260	3846	100 ± 50	ν(C=C)
270	3704	100 ± 50	ν(C=C)
280	3571	100 ± 50	ν(C=C)
290	3448	100 ± 50	ν(C=C)
300	3333	100 ± 50	ν(C=C)
310	3226	100 ± 50	ν(C=C)
320	3125	100 ± 50	ν(C=C)
330	3029	100 ± 50	ν(C=C)
340	2938	100 ± 50	ν(C=C)
350	2851	100 ± 50	ν(C=C)
360	2768	100 ± 50	ν(C=C)
370	2689	100 ± 50	ν(C=C)
380	2614	100 ± 50	ν(C=C)
390	2542	100 ± 50	ν(C=C)
400	2473	100 ± 50	ν(C=C)

TABLE I (continued)

COMPARISON OF EXCITED STATES OF  $\text{Co}^{60}$  (Kev)

<u>Peak</u>	<u>Present Work</u>	<u>Bartholomew and Kinsey</u>	<u>Rateson and Pollard</u>
1	60 $\pm$ 3		
2	286 $\pm$ 3	285*	390
3	445 $\pm$ 3	445*	
4	513 $\pm$ 3	512*	
5	557 $\pm$ 5		
6	621 $\pm$ 4	619*	
7	792 $\pm$ 3	796*	810
8	1012 $\pm$ 3	1012*	
9	1237 $\pm$ 5	1236	1280
10	1394 $\pm$ 4	1376	
11	1533 $\pm$ 6	1520	
12	1663		
		1760	1730
13	1825	1840	
14	2002		
15	2061		
16	2154	2135	2170
17	2292	2307	
18	2370		
19	2615	2583	
20	2630		

TABLE IV

(1987) 10/25 72 000000 000000 000000

Account Number	Account Number	Account Number	Account Number
		100000	1
1000	1000	100000	2
	1000	100000	3
	1000	100000	4
	1000	100000	5
1000	1000	100000	6
	1000	100000	7
	1000	100000	8
1000	1000	100000	9
	1000	100000	10
	1000	100000	11
	1000	100000	12
1000	1000	100000	13
	1000	100000	14
	1000	100000	15
1000	1000	100000	16
	1000	100000	17
	1000	100000	18
1000	1000	100000	19
	1000	100000	20
	1000	100000	21
	1000	100000	22
	1000	100000	23
	1000	100000	24
	1000	100000	25
	1000	100000	26
	1000	100000	27
	1000	100000	28
	1000	100000	29
	1000	100000	30

<u>Peak</u>	<u>Present Work</u>	<u>Bartholomew and Kinsey</u>	<u>Bateson and Pollard</u>
21	2791		
22	2871		
23	2924	2900	
24	3038		
		3120	
25	3211		
26	3309	3300	
		3460	
		3800	
		4130	
27	4226		
28	4306		
29	4425		
30	4571		

\*Levels whose existence is inferred from strong  
homogeneous gamma rays.

TABLE IV  
(Continued)

Account No.	Description	Amount	Total
		1000	1000
		2000	2000
		3000	3000
		4000	4000
		5000	5000
		6000	6000
		7000	7000
		8000	8000
		9000	9000
		10000	10000
		11000	11000
		12000	12000
		13000	13000
		14000	14000
		15000	15000
		16000	16000
		17000	17000
		18000	18000
		19000	19000
		20000	20000
		21000	21000
		22000	22000
		23000	23000
		24000	24000
		25000	25000
		26000	26000
		27000	27000
		28000	28000
		29000	29000
		30000	30000
		31000	31000
		32000	32000
		33000	33000
		34000	34000
		35000	35000
		36000	36000
		37000	37000
		38000	38000
		39000	39000
		40000	40000
		41000	41000
		42000	42000
		43000	43000
		44000	44000
		45000	45000
		46000	46000
		47000	47000
		48000	48000
		49000	49000
		50000	50000
		51000	51000
		52000	52000
		53000	53000
		54000	54000
		55000	55000
		56000	56000
		57000	57000
		58000	58000
		59000	59000
		60000	60000
		61000	61000
		62000	62000
		63000	63000
		64000	64000
		65000	65000
		66000	66000
		67000	67000
		68000	68000
		69000	69000
		70000	70000
		71000	71000
		72000	72000
		73000	73000
		74000	74000
		75000	75000
		76000	76000
		77000	77000
		78000	78000
		79000	79000
		80000	80000
		81000	81000
		82000	82000
		83000	83000
		84000	84000
		85000	85000
		86000	86000
		87000	87000
		88000	88000
		89000	89000
		90000	90000
		91000	91000
		92000	92000
		93000	93000
		94000	94000
		95000	95000
		96000	96000
		97000	97000
		98000	98000
		99000	99000
		100000	100000



clear that Bartholomew and Kinsey were measuring gamma-rays to the ground state of  $\text{Co}^{60}$ , not to the metastable state. They state<sup>3</sup> that, should this be the case, the intensity of gamma-rays to the metastable state is less than 10 percent of those to the ground state.

As an explanation for this, it is noted that there is a resonance in the  $\text{Co}^{59}$  neutron capture cross section at 123 ev, which state presumably influences the capture of thermal neutrons if we make the reasonable assumption<sup>15</sup> that the energy level spacing here is of the order of tens of kilovolts. It is reasonable further to assume, then, that s-wave neutrons are captured into the (f)  $7/2$  ground state of  $\text{Co}^{59}$  to form a  $4-$  state, and that electric dipole radiation to the  $5+$  ground state of  $\text{Co}^{60}$  exceeds the magnetic quadrupole radiation to the  $2+$  metastable state by a factor greater than 10.

The level density as presented in Figure 8 is, unfortunately, not conclusive, as it is felt that in the region of excitation above 1 Mev there are some  $\text{Co}^{60}$  levels whose intensities are not sufficiently high uniquely to identify them as such. Above an excitation of 4.8 Mev, no useful information was obtained on level densities. A lower limit on level densities below this figure is set, however, and it is easily seen by comparison with Bartholomew and Kinsey's gamma spectra of iron and nickel that this odd-odd nucleus has a more complex spectrum than that of its even-odd neighbors.

The first part of the paper is devoted to a study of the
 asymptotic behavior of the  $n$ -th order statistic  $X_{(n)}$ 
 of a sample of size  $n$  from a distribution with density
  $f(x)$  and cumulative distribution function  $F(x)$ .
 It is assumed that  $f(x)$  is continuous and that
  $F(x)$  is strictly increasing. The main result of
 this part is the following theorem:

Let  $X_1, X_2, \dots, X_n$  be a random sample of size
  $n$  from a distribution with density  $f(x)$  and
 cumulative distribution function  $F(x)$ . Let
  $X_{(n)}$  be the  $n$ -th order statistic. Then,
 as  $n \rightarrow \infty$ ,

$$\frac{X_{(n)} - F^{-1}(1/n)}{F^{-1}(1/n)} \rightarrow 0$$

in probability. This result shows that the
  $n$ -th order statistic is asymptotically
 equivalent to the inverse of the cumulative
 distribution function evaluated at  $1/n$ .

The second part of the paper is devoted to a study
 of the asymptotic behavior of the  $k$ -th order
 statistic  $X_{(k)}$  of a sample of size  $n$  from
 a distribution with density  $f(x)$  and cumulative
 distribution function  $F(x)$ . It is assumed that
  $f(x)$  is continuous and that  $F(x)$  is
 strictly increasing. The main result of this
 part is the following theorem:

Let  $X_1, X_2, \dots, X_n$  be a random sample of
 size  $n$  from a distribution with density
  $f(x)$  and cumulative distribution function
  $F(x)$ . Let  $X_{(k)}$  be the  $k$ -th order
 statistic. Then, as  $n \rightarrow \infty$ ,

$$\frac{X_{(k)} - F^{-1}(k/n)}{F^{-1}(k/n)} \rightarrow 0$$

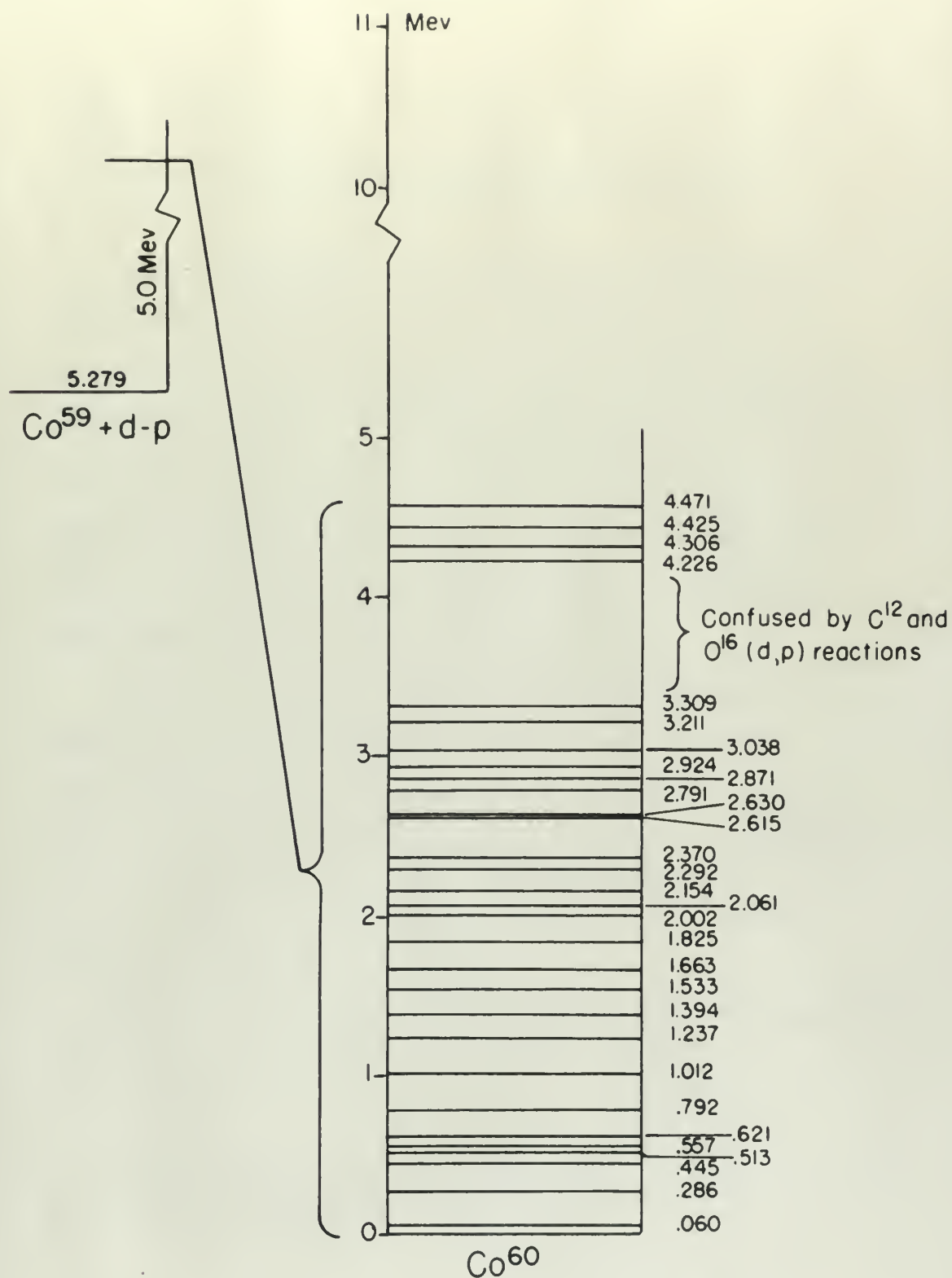
in probability. This result shows that the
  $k$ -th order statistic is asymptotically
 equivalent to the inverse of the cumulative
 distribution function evaluated at  $k/n$ .

The third part of the paper is devoted to a study
 of the asymptotic behavior of the  $k$ -th order
 statistic  $X_{(k)}$  of a sample of size  $n$  from
 a distribution with density  $f(x)$  and cumulative
 distribution function  $F(x)$ . It is assumed that
  $f(x)$  is continuous and that  $F(x)$  is
 strictly increasing. The main result of this
 part is the following theorem:

Let  $X_1, X_2, \dots, X_n$  be a random sample of
 size  $n$  from a distribution with density
  $f(x)$  and cumulative distribution function
  $F(x)$ . Let  $X_{(k)}$  be the  $k$ -th order
 statistic. Then, as  $n \rightarrow \infty$ ,

$$\frac{X_{(k)} - F^{-1}(k/n)}{F^{-1}(k/n)} \rightarrow 0$$

in probability. This result shows that the
  $k$ -th order statistic is asymptotically
 equivalent to the inverse of the cumulative
 distribution function evaluated at  $k/n$ .



ENERGY LEVELS IN  $Co^{60}$

Figure 8





## APPENDIX 4

Proposal for the Determination of the Spin of  $\text{Co}^{60}$ 

The accepted values<sup>1</sup> of the spins and parities of the ground and first excited states of  $\text{Co}^{60}$  are  $5+$  and  $3+$ , respectively. The discovery of a newly discovered beta from the ground state of  $\text{Co}^{60}$  to the first excited state of  $\text{Ni}^{60}$  leads Keister and Schmidt<sup>2</sup> to assign values of  $4+$  and  $1+$ , respectively, to the above levels, although such assignments cannot be reconciled with the lack of a beta decay from the first excited state of  $\text{Co}^{60}$  to the ground state of  $\text{Ni}^{60}$ .

In order to attempt to resolve this question it is proposed that the new magnetic spectrometer be used to measure the angular distribution from  $0^\circ$  to  $120^\circ$  of protons from the  $\text{Co}^{59}(d,n)\text{Co}^{60}(0.054)$  reaction, utilizing Butler's<sup>3</sup> theory of angular distribution as a function of the angular momentum  $l$  of the captured neutron.

The shell model and Schmidt diagram concur in assigning odd parity to the ground state of  $\text{Co}^{59}$  ( $I = 7/2$ ), so one

1. Goldhaber and Hill, *PR*, 2, 179, (1952)
2. Keister and Schmidt, *PR*, 11, 148, (1954)
3. Butler, *PR*, 1, 550, (1951)



CHAPTER IV

THEORY OF THE DIFFERENTIAL EQUATIONS

The theory of differential equations is a branch of mathematics that deals with the study of functions and their derivatives. It is one of the most important and useful branches of mathematics, and it has many applications in science, engineering, and economics.

The basic idea of a differential equation is to relate a function to its derivative. For example, the equation  $y' = ky$  describes the growth of a population, where  $y$  is the population and  $k$  is the growth rate. The equation  $y'' + y = 0$  describes the motion of a simple harmonic oscillator, where  $y$  is the displacement and  $y''$  is the acceleration.

There are many different types of differential equations, and they are classified according to their order, linearity, and other properties. The most common types are ordinary differential equations (ODEs) and partial differential equations (PDEs). ODEs are equations that involve only one independent variable, while PDEs involve two or more independent variables.

The theory of differential equations is a rich and complex subject, and it has many interesting results and techniques. One of the most important results is the existence and uniqueness theorem, which states that under certain conditions, a differential equation has a unique solution. Another important result is the method of separation of variables, which is used to solve many types of differential equations.

The theory of differential equations is also closely related to other branches of mathematics, such as calculus, algebra, and geometry. For example, the theory of differential equations is used to study the properties of functions and their graphs, and it is used to solve problems in geometry and physics.

THEORY OF THE DIFFERENTIAL EQUATIONS  
 PART I. ORDINARY DIFFERENTIAL EQUATIONS  
 CHAPTER I. FIRST-ORDER DIFFERENTIAL EQUATIONS

would expect the orbital angular momentum of the neutron,  $l_n$ , captured in going to the first excited state of  $^{60}\text{Co}$  to be 1 or 3. If  $l_n$  were found to be 1 it would rule out the assignment of 1- to the first excited state of  $^{60}\text{Co}$ , whereas if  $l_n = 3$ , both 1- and 2- are allowed states of this level.

Using deuterons of 6.4 Mev energy in c.m.s. ( $6.4 \times 61/59 = 6.6$  Mev in laboratory system) and an outgoing c.m.s. energy of  $6.4 - 5.23 = 11.63$  Mev, it is clear from the figures in Butler's article that the differential cross-section for the reaction could peak at about  $22^\circ$  for  $l_n = 1$ ,  $3^\circ$  for  $l_n = 2$ , and  $51^\circ$  for  $l_n = 3$ , all angles in c.m.s.

In order to convert laboratory system angles to c.m.s. one must add to the measured angles,  $\theta$ , the quantity  $(\Theta - \theta)$ , where

$$\begin{aligned} \sin(\Theta - \theta) &= \frac{\sin \theta \times \text{vel of c. of m.}}{\text{vel of proton in c. of m.}} \\ &= \frac{\sin \theta \sqrt{\frac{2E_d}{m_d}} \quad 2/61}{\sqrt{\frac{2}{m_d}} (11.63 \text{ Mev}) 60/61} \\ &= \sin \theta \sqrt{\frac{6.6}{2 \times 11.63} \frac{61}{60} \frac{2}{61}} \\ &= .0176 \sin \theta \quad [(\Theta - \theta) = 1.0^\circ \text{ at } \theta = 90^\circ] \end{aligned}$$

... the ... of the ...  
 ... the ... of the ...  
 ... the ... of the ...  
 ... the ... of the ...  
 ... the ... of the ...  
 ... the ... of the ...  
 ... the ... of the ...  
 ... the ... of the ...  
 ... the ... of the ...  
 ... the ... of the ...  
 ... the ... of the ...  
 ... the ... of the ...

$$(\theta - \theta)$$

$$\frac{\partial \theta}{\partial \theta} = \theta - \theta$$

$$\frac{\partial \theta}{\partial \theta} = \theta - \theta$$

$$\frac{\partial \theta}{\partial \theta} = \theta - \theta$$

$$[\theta = \theta \text{ or } \theta = (\theta - \theta)] \theta \text{ or } \theta = \theta$$

## BIBLIOGRAPHY

1. J. A. Harvey, Phys. Rev. 81, 353 (1951).
2. J. A. Harvey, Can. J. Phys. 31, 278 (1953).
3. G. A. Bartholomew and B. W. Winsey, Phys. Rev. 89, 386 (1953).
4. G. L. Keister and F. E. Schmidt, Phys. Rev. 93, 140 (1954).
5. R. L. Caldwell, Phys. Rev. 78, 407 (1950).
6. W. D. Bateson and E. Pollard, Phys. Rev. 79, 241 (1950).
7. D. C. Hoesterey, Phys. Rev. 87, 216 (1952).
8. J. M. Hollender, I. Perlman, and G. T. Seaborg,  
Revs. Modern Phys. 25, 469 (1953).
9. S. T. Butler, PRS (London), A-208, 559 (1951).
10. E. N. Strait, PhD Thesis, Physics Department, MIT (1948).
11. E. N. Strait, D. W. Van Patter, W. W. Buechner, and  
A. Sperduto, Phys. Rev. 81, 747 (1951).
12. J. E. Schwager and I. A. Cox, Rev. Sci. Instr. 24, 986, (1953).
13. H. A. Ruge, Rev. Sci. Instr. 23, 599 (1952).
14. M. M. Elkind, PhD Thesis in Physics, MIT (1951).
15. E. Segre, Ed., Exp. Nuc. Phys., Vol. II, 264 (1953).



CONTENTS

- 1. A. A. ... (1921)
- 2. A. A. ... (1922)
- 3. A. A. ... (1923)
- 4. A. A. ... (1924)
- 5. A. A. ... (1925)
- 6. A. A. ... (1926)
- 7. A. A. ... (1927)
- 8. A. A. ... (1928)
- 9. A. A. ... (1929)
- 10. A. A. ... (1930)
- 11. A. A. ... (1931)
- 12. A. A. ... (1932)
- 13. A. A. ... (1933)
- 14. A. A. ... (1934)
- 15. A. A. ... (1935)

















28812  
Foglesong  
Energy levels in Co<sup>60</sup>.

28812  
Foglesong  
Energy levels in Co<sup>60</sup>.

thesF53

Energy levels in Co(60) /



3 2768 001 96820 9

DUDLEY KNOX LIBRARY